Microscopic Complexity in Phase-Change Materials and its Role for Applications

*Volker L. Deringer, Richard Dronskowski, and Matthias Wuttig**

Phase-change materials (PCMs) are widely used for data storage and in other functional devices. Despite their seemingly simple compositions, these materials exhibit intriguing microscopic complexity and a portfolio of interesting properties. In this Feature Article, it is shown that structural and electronic peculiarities on the atomic scale are key determinants for the technological success of PCMs. Particular emphasis is put on the interplay of different experimental and theoretical methods, on the bonding nature of crystalline and amorphous PCMs, and on the role of surfaces and nanostructures. Then, unconventional transport properties of the crystalline phases are highlighted, both with regard to electrical and heat conduction. Finally, perspectives and future directions are drawn: for finding new PCMs based on microscopic understanding, and also for new applications of these materials in emerging fields.

1. Introduction

The ability to preserve and process information has shaped the development of society ever since. The advent of digital technology (and thus of "ones" and "zeroes") has sped up the pace, has made everyday life easier in many regards, but also introduced new challenges. The density of data is increasing, but so is their fleeting nature; established memory concepts such as Flash technology are progressively approaching the limits of how much information they can handle, and for how long data can be stored. Physicists, chemists, and materials scientists are hence needed to find new ingredients for data-storage and data-processing technologies.

Phase-change materials (PCMs) are among the most promising candidates in this regard. They are used by industry, for example, in re-writeable Blu-Ray disks, and at the same time by academia for numerous new applications. The underlying principle was proposed by Ovshinsky in 1968 already:[1] a PCM takes two solid-state phases of distinctly different physical properties, which can be used to encode one and zero bits, and rapidly switched back and forth (**Figure 1**).

An ingenious idea at first, phase-change data storage saw a fundamental breakthrough a quarter of a century ago, when quasibinary GeTe–Sb_2Te_3 alloys were discovered to be suitable for optical storage.[3] More recently, the focus shifted back toward electronic memories,[4] building on wholly different physical principles (a contrast in conductivity rather than reflectivity) but on the same ingredients as the aforementioned optical disks. Most prominently, the "DVD-RAM material" $Ge_2Sb_2Te_5$ is now widely used for electrical switching.[5] This fact already emphasizes how versatile—and special—these materials are.

Remarkably indeed, PCMs continue to pose challenges (and exciting opportunities) for very basic fundamental research. This is because they differ strongly from "textbook" solids such as, say, crystalline and amorphous silicon. **Table 1** summarizes a number of characteristic properties for both, which will be relevant throughout this work and discussed in the oncoming sections. The conundrum goes even further: what is a phase-change material? Thermoelectrics, for example, are assessed by their figure of merit *ZT* (the thermoelectric community may forgive us for this simplification); for phase-change data storage, on the other hand, there is no comparable, clear-cut quality criterion, but rather an entire catalogue of different requirements.[2,6] Take antimony telluride (Sb_2Te_3): it is chemically almost indistinguishable from $GeSb_4Te_7$, but the binary compound crystallizes too readily and cannot be kept in the amorphous state under practical conditions. Other materials may be switchable but lack the required property contrast. We finally note in passing that the term "phase-change material" is also used in different contexts, such as latent-heat storage,[7] but this will not be the topic here.

There have been previous, excellent reviews by others that focus on technological applications of PCMs. We may refer the reader to the literature for an introduction to nonvolatile memory technology ("phase-change RAM"),[9] and for a comprehensive account on this matter;[10] the latter is particularly interesting in that it comes from an industrial perspective, other than this one. Glass physics—a crucial aspect for the amorphous "zero bits"—has been covered in previous reviews by one of us (M.W.).[2,6] There are also specialized textbooks

Dr. V. L. Deringer, Prof. R. Dronskowski
Institute of Inorganic Chemistry
RWTH Aachen University
Landoltweg 1, 52056 Aachen, Germany
Prof. R. Dronskowski, Prof. M. Wuttig
Jülich–Aachen Research Alliance (JARA-FIT and JARA-HPC)
RWTH Aachen University
52056 Aachen, Germany
E-mail: wuttig@physik.rwth-aachen.de
Prof. M. Wuttig
Institute of Physics IA
RWTH Aachen University
52056 Aachen, Germany

DOI: 10.1002/adfm.201500826

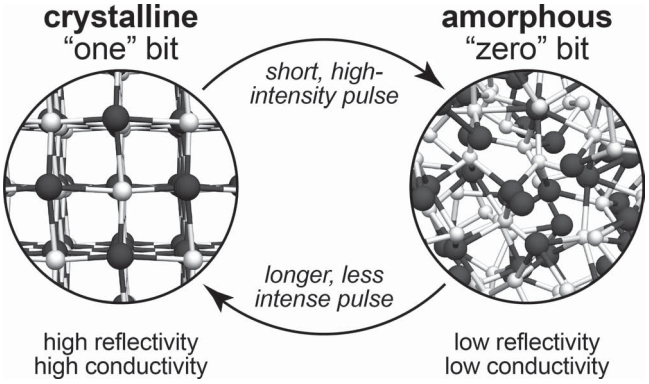

Figure 1. The functional principle of phase-change data storage.[2] Ones and zeroes are encoded by small bits of a PCM (here exemplified by the binary GeTe) which differ strongly in their physical properties. In optical storage media such as the re-writeable Blu-Ray disk, the materials are switched by laser pulses, and the contrast in reflectivity is read out to retrieve the digital information. In electronic media, current pulses (and thus Joule heating) are employed; in this case, the different conductivities of the crystalline and amorphous phase encode the ones and zeroes.

which expand further than would be possible here.[5,11] In this Feature Article, we will focus on the atomistic nature of PCMs, highlighting intriguing peculiarities and recent successes, and we will show how macroscopic applications (and possible new perspectives) emerge from such very fundamental microscopic properties.

2. Structural Complexity in "Simple" Tellurides

This work aims to identify microscopic effects that make PCMs technologically important. At the outset of this endeavor, it is imperative to understand the compounds' atomic structures as well as possible. There are still unresolved issues and challenges, even more so as different experimental (and theoretical) techniques may lead to different structural descriptions, and a well-rounded picture requires several probes. In this section, we review aspects, as known to date, of the atomic arrangements in crystalline and amorphous PCM bits.

2.1. The Ideal Crystalline Phases: Similarities at Second Sight

Germanium telluride (GeTe) was presented as the prototype PCM in the Introduction, and rightfully so: having been built into phase-change devices itself,[12] it also forms the starting point of the GeTe–Sb_2Te_3 quasibinary line. Here, it will serve us as the structural parent from which all other compounds can be derived, at least in principle.

The first synthesis of GeTe, achieved by fusing the elements, was reported in the 1930s already,[13] and the crystal structure was described in 1951.[14] A distorted rocksalt-like modification ("α-GeTe") was found at ambient conditions, and the structure was subsequently refined in the rhombohedral spacegroup $R3m$ based on X-ray[15] and neutron diffraction.[16] In the ideal rocksalt type, both cations and anions are octahedrally, that is, perfectly sixfold coordinated. The resulting octahedra are stacked along the [111] direction, giving rise to alternating cation and anion layers with equidistant spacing. In α-GeTe, a slight rhombohedral distortion shifts these layers with regard to one another, and thus the sixfold coordination becomes "3+3"-fold; concomitantly, the cell angle is lowered by a few degrees compared to the ideal rocksalt type.[15,16] **Figure 2** offers two possible ways of describing the α-GeTe structure. The left-hand side emphasizes the proximity to the conventional rocksalt cell, using the $F13m$ setup as von Schnering and co-workers have

Volker Deringer studied chemistry at RWTH Aachen University as a fellow of the German National Academic Foundation. He obtained his diploma in 2010 and his doctorate in 2014, working under guidance of Richard Dronskowski on the quantum-chemical modeling and theory of complex solid-state materials (including PCMs). Volker is curious about the chemical-bonding nature of solids, including surfaces, defects, molecular crystals, and amorphous matter.

Richard Dronskowski studied chemistry and physics in Münster and received his doctorate under guidance of Arndt Simon in Stuttgart, in 1990. After a stay as a guest scientist with Roald Hoffmann, he obtained his habilitation in Dortmund and, since 1997, holds the Chair of Solid-State and Quantum Chemistry at RWTH Aachen University. His research interests span synthetic solid-state chemistry, neutron diffraction, and the quantum theory and simulation of solid materials.

Matthias Wuttig studied physics in Köln (Cologne) and received his doctorate under guidance of Harald Ibach working at the Jülich research center. After stays as guest scientist at Lawrence Berkeley Laboratory and AT&T Bell Labs, he joined RWTH Aachen University in 1997, where he holds the Chair for Physics of Novel Materials. His research interests include materials with unconventional electronic and optical properties.

Table 1. Characteristic properties of a textbook semiconductor (silicon) and of a prototypical phase-change data-storage material (GeTe): both solid-state phases of the latter are "special" in many regards. Adapted from the literature.[8]

	Amorphous Si	Crystalline Si	Amorphous GeTe	Crystalline GeTe
Atomic coordination	tetrahedral (8–*N* rule)	tetrahedral (8–*N* rule)	different co-existing motifs	distorted octahedral
Bonding nature	textbook covalent		covalent	"resonant" bonding
Thermal conductivity	low	high	low	low
Optical reflectivity	low contrast		high contrast	
Electrical conductivity	low	*p*- or *n*-type doping possible	low	*p*-type through self-doping

done;[16] the right-hand side outlines the stacking of octahedra along the crystallographic [111] direction, and the alternation of short and longer bonds which leads to the formation of Ge–Te bilayers. One or the other model can—and should—be chosen, depending on the particular task at hand.

At high temperature, GeTe departs from the structure shown above. A second-order phase transition to an undistorted rocksalt-type modification has traditionally been assumed ("α-GeTe $\rightarrow$ β-GeTe"), which implies an equalization of the "short" and "longer" Ge–Te bonds above $\approx$ 430 °C.[16] The transition temperature had earlier been seen to depend on minute variations in the sample composition and spans a broad range,[14] which is unusual for precisely defined textbook crystals: take the $\alpha \rightarrow \beta$ transition in quartz, which occurs precisely at 573 °C.[18] Apparently, GeTe is more complex than its simple formula suggests. More recently, it was argued that the observed "ideal" rocksalt structure results from averaging effects whereas the local atomic environment (invisible to Bragg diffraction) and thus the Ge–Te bond lengths stay quite unaffected, even at high temperature.[19] The origin of this apparent discrepancy lies in the different measurement techniques: X-ray and neutron diffraction yield the global structure whereas EXAFS probes the local surrounding of the atoms; all experiments are right in themselves, and the nature of the phase transition is still under discussion as of today.[20] The influence of different experimental probes (and the importance of looking at local effects, too) is a recurring theme in structural studies of PCMs, as nicely illustrated by this example.

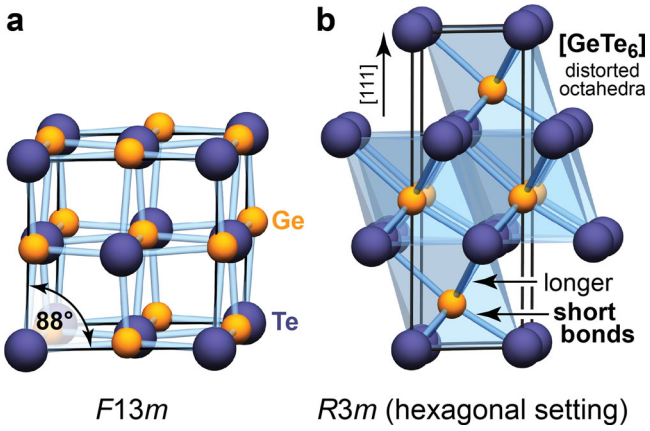

Figure 2. a) Crystal structure of α-GeTe in the "quasi-rocksalt" description with *F*13*m* symmetry and a cell angle slightly below 90°.[17] b) Same structure but in hexagonal setting (note that the space-group symmetry is not hexagonal due to the presence of a threefold, rather than sixfold, rotation axis). This way, the distorted octahedral coordination environment is best seen, as is the stacking of alternating Ge and Te layers along the rhombohedral [111] (≡ hexagonal [0001]) direction.

The other end member of the quasibinary line is antimony telluride, Sb_2Te_3; it is not employed in current phase-change applications itself, due to its unsuitable crystallization temperature (see above), but constitutes an important parent compound nonetheless. Sb_2Te_3 crystallizes in a well-ordered sequence of layered structural units,[21] terminated by Te planes and stacked on top of each other (**Figure 3**); Te···Te contacts hold the building blocks together, which are often termed as van-der-Waals (vdW) type contacts, and this assignment can be corroborated by the low interlayer energy (see below). At second sight, the crystal structures of GeTe and Sb_2Te_3 are closely related: the Te···Te motif is absent in GeTe (which instead consists of alternating Ge and Te layers throughout), but the 2D layers themselves are similar, as are the crystal symmetries and in-plane lattice parameters. Formally, one may thus "mix" GeTe and Sb_2Te_3 to arrive at the idealized layered structures of the quasibinaries, as outlined before.[22]

The structure determination of layered tellurides is a challenging task and often impossible in "laboratory-grade" diffraction experiments; the interested reader is referred to an in-depth technical account in a previous study.[24] The stacking sequence in the layered phases, that is, the distribution of Ge, Sb, and vacancies between the dense tellurium layers, is a prime example which has long been unresolved even for the comparably simple $Ge_2Sb_2Te_5$. The crystal structure of the latter was initially explored by electron diffraction, which led to a first stacking model with all Ge atoms residing on 2*c* sites adjacent to the Te···Te layers, and all Sb on 2*d* sites inside the building blocks.[25] Later, Kooi and De Hosson revised the stacking sequence based on high-resolution transmission electron microscopy (HRTEM),[26] inverting the cation ordering ("Sb outside") to give what is sketched in Figure 3. A number of careful synchrotron studies have subsequently been reported for different PCMs from the GeTe–Sb_2Te_3 tieline.[27] From these experiments on $Ge_2Sb_2Te_5$,[27b] mixed occupations were finally deduced, with the majority of Sb residing near the Te···Te layers. The driving force for these is, in part, a simple matter of mixing entropy.

Density-functional theory (DFT) simulations have become an indispensable part of materials modeling, being, today, a "mature" counterpart and complement to many experimental techniques.[28] As such, they are frequently applied to investigate PCMs. Layered $Ge_2Sb_2Te_5$ is an instructive example. Model DFT computations of the stacking sequence confirmed the

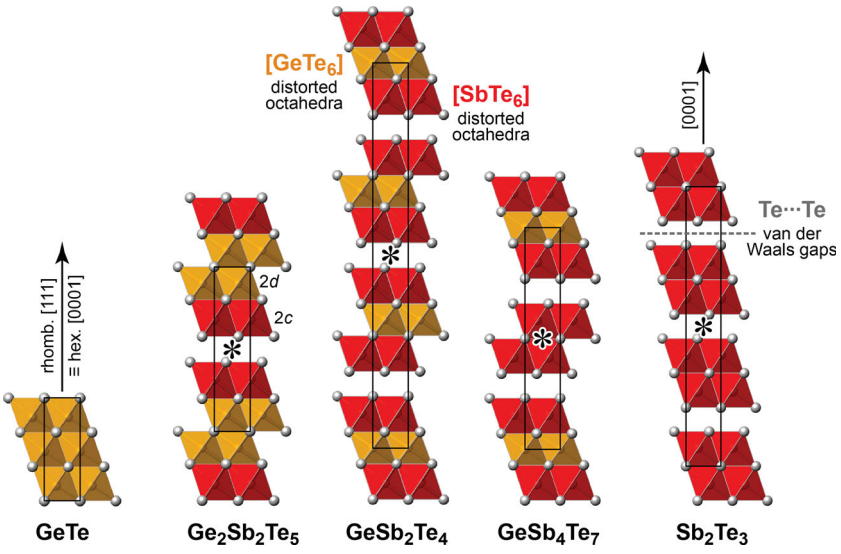

Figure 3. Idealized crystal structures along the GeTe–Sb_2Te_3 tieline in polyhedral representation; the Sb content increases from left to right. For $Ge_2Sb_2Te_5$, Wyckoff labels (2*c*/2*d*) are given for the two inequivalent cation sites; in reality, intermixing of Ge and Sb atoms is to be expected, as discussed in the text. All phases except GeTe take inversion-symmetric space groups, and the inversion centers have been highlighted by asterisks (*). Figure created using VESTA.[23]

tendency proposed by Kooi and De Hosson[29] and, at the same time, iconized the very nature of the problem: quantum-theoretical structure models are necessarily small and discretized; they can never fully capture reality (e.g., the fractional occupation factors), and theorists must come up with models as representative as possible.[22] Just as well, structural drawings such as those in Figure 3 are mostly simplified and depict "balls and sticks" rather than the partial occupation factors afforded by careful experiments. This does not hamper their usefulness—quite on the contrary so.

The reader may have noticed that the discussion has so far been concerned with one major family of PCMs exclusively. There is another, namely, Ag/In doped Sb_2Te ("AIST"), discovered around the same time as $Ge_2Sb_2Te_5$[30] and likewise used in industry.[2] We will do AIST injustice here and only mention it in passing, to keep this article concise. Stoichiometrically precise Sb_2Te takes a well-ordered layered structure[31] closely related to Sb_2Te_3: there are quintuple-layer building blocks, too, and between them one finds corrugated double layers that consist purely of Sb atoms (and thus resemble the crystalline structure of the element). This principle of alternating building blocks, with weak vdW forces in between, is again representative of a larger range of long periodic stacking structures: the binary Sb–Te phase diagram is complex indeed.[32] Pure Sb_2Te, however, is unsuitable as a PCM, as it crystallizes too easily. To counteract this problem, a few percent of guest atoms are introduced, leading to the aforementioned AIST material whose structure has been discussed in detail elsewhere.[5,11,33]

Layered tellurides from the aforementioned families exhibit large unit-cell vectors and thus long periodicities along [0001]. These structures have recently become important for applications reliant on precise atomic ordering (Section 5). For present-day commercial devices such as Blu-Ray disks, on the other hand, the ideally layered compounds are much less relevant; the rapid switching times do not allow the crystalline phase to reach thermal equilibrium and orderly arrange themselves into layers. Instead, we now turn to metastable Ge–Sb–Te alloys which take the defective rocksalt type.

2.2. Metastable (Rocksalt-Type) Phases

At first sight, rocksalt-type Ge/Sb tellurides do not seem to have much in common with their stable layered counterparts. A closer look, however, reveals that both are intimately related—and that there is a gradual transition between both.

The simplest possible structural model was derived from X-ray diffraction:[3b,27b] Te atoms form a fully occupied anionic sublattice, whereas Ge and Sb atoms as well as vacancies are randomly distributed on the cationic one. Once more, one may alternatively use the pseudo-hexagonal cell setup (akin to Figure 2b): therein, the metastable phases can be described as dense Te-filled planes alternating with disordered layers (containing 40% Ge, 40% Sb, and 20% vacancies each), again stacked along the [111] direction.[27b] This model is now widely accepted and provides the key mnemonic for understanding metastable crystalline PCMs.

Closer inspection, however, reveals that the inherently assumed complete disorder on the cationic sublattice is again a simplification. Important further insight was recently gained by electron microscopy (and diffraction) studies on carefully prepared metastable Ge–Sb–Te alloys.[34] **Figure 4**a shows two representative HRTEM images for the GeTe-rich quasi-binary phase $(GeTe)_{12}(Sb_2Te_3)$.[34a] If this compound is rapidly quenched, canted vacancy layers emerge, as seen on the left-hand side. Allowing the sample, instead, to anneal for several hours before quenching, one observes parallel vacancy layers with irregular spacing (right-hand side). In thermal equilibrium, the vacancies finally form precisely defined and equidistant planes. This sequence of progressive vacancy ordering has been sketched in Figure 4b, and it illustrates the step-by-step transition from fully disordered (left-hand side) to fully ordered (right-hand side). Such progressive ordering of vacancies will become crucial later when discussing the charge transport in PCMs (Section 4).

2.3. From the Bulk to Surfaces and Nanostructures

Phase-change memory devices are becoming smaller and smaller, nowadays down to the nanoscale: one can readily manufacture phase-change films a few ten atomic layers thick. This impacts the physical properties—for example, it strongly increases the crystallization temperatures as compared to bulk samples of the same material,[35] and it naturally promises to increase the information density. Given the current surge of

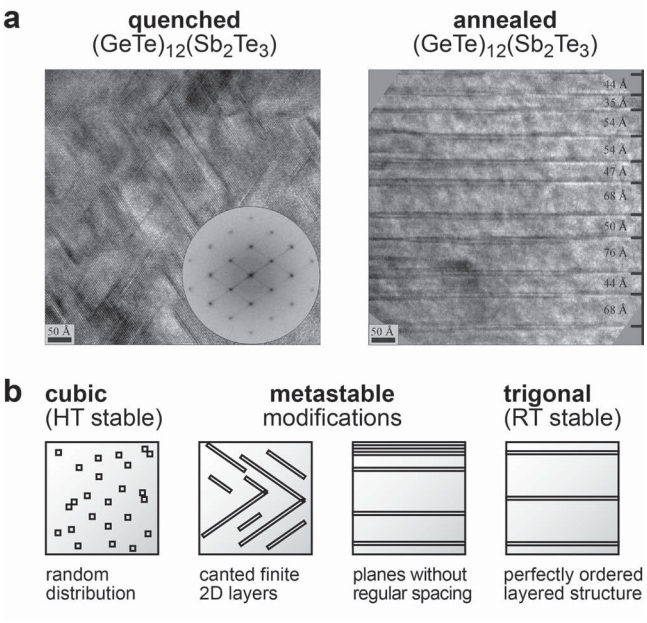

Figure 4. a) HRTEM images of metastable crystallized $(GeTe)_{12}(Sb_2Te_3)$ samples; left: quenched from 500 °C (with Fourier transformation in the inset); right: annealed at 400 °C for 20 h and subsequently quenched, with the spacing of vacancy layers indicated. Reprinted figure with permission by the American Physical Society.[34a] Copyright 2010. b) Schematic sketch of different vacancy distributions in these GeTe-rich phases. Adapted with permission by the Royal Society of Chemistry.[34c] Copyright 2012.

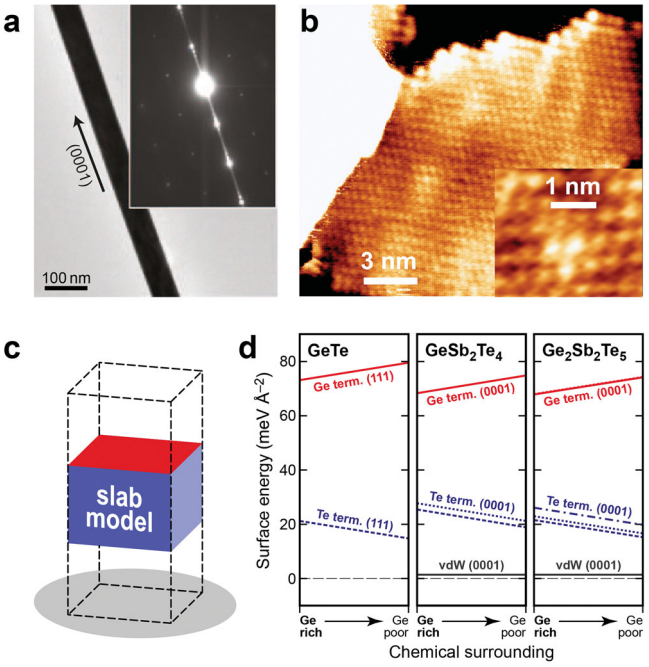

Figure 5. a) TEM image of a $Ge_2Sb_2Te_5$ nanowire. The inset shows the electron-diffraction pattern, confirming single-crystallinity. Reprinted by permission.[37] Copyright 2007, The Authors. b) STM images of $Ge_2Sb_2Te_5$(111) surfaces; the atom-resolved close-up reveals dense 2D layers of atoms. Reprinted with permission.[38] Copyright 2013, AIP Publishing LLC. c) Schematic DFT slab model for simulating material surfaces, with the boundaries of the simulation cell indicated by dashed lines. d) DFT-GGA computed surface phase diagrams for GeTe(111) and for related quasibinary (0001) surfaces, comparing the stabilities of competing terminations. The surface energies for the "van der Waals" type surfaces are higher if dispersion corrections to DFT are incorporated, but the qualitative results are unaffected. Adapted with permission.[50] Copyright 2013, American Chemical Society.

interest in nanostructures, it is worth noting that thin films of GeTe (down to 8 nm in thickness) have been prepared, and their properties elucidated by techniques including TEM, almost half a century ago already.[36] Since then, significant strides have been made both with regard to synthesis and characterization techniques. In the recent years, a plethora of nanostructures, nanowires etc. have been reported, one of which is shown in **Figure 5**a.[37]

Nanoparticles are naturally influenced by their surfaces to a significant degree: reducing the length of a cubic particle from one millimeter down to 10 nm increases its surface-to-volume ratio by five orders of magnitude. It is possible, nowadays, to create atomically resolved pictures of these surfaces; an example is shown in Figure 5b and has been obtained by scanning tunneling microscopy (STM).[38] Such investigations, truly on the atomic scale, open the ground for fruitful combinations of theory and experiment: the different length scales of both, hitherto several orders of magnitude apart, are progressively approaching each other.

Let us start again by looking at GeTe. To identify the most important surfaces of a given material, one will ask for the morphology and habit of its crystals: think of table salt with its characteristic cubic crystallites that expose {001} facets exclusively. Upon resublimation in vacuum, GeTe forms crystals of near-perfect octahedral morphology;[39] such crystal shape, in rocksalt-type compounds, is controlled by the {111} facets. This is understandable if looking at the crystal structure, which consists of Ge–Te bilayers extending in the {111} planes (Figure 2b): it seems reasonable to assume that the crystal is cleaved between the bilayers, thereby keeping all short (and strong) Ge–Te bonds intact.[40]

Such hypotheses may now be tested by atomistic simulations. To simulate surfaces by means of DFT, one "cleaves" properly oriented, periodic slabs from the bulk crystal structure; previous work is recommended for a general introduction to ab initio surface science.[41] The sketch in Figure 5c outlines surfaces (red) exposed at the top and bottom of such a slab model, terminated by artificial vacuum regions perpendicular to the surface. Performing DFT computations on this model yields optimized structures (for comparison to experiments like STM) and, conveniently, stabilities: the latter are expressed by surface energies, denoted γ, which measure the energetic cost of a given surface relative to the bulk.[41]

Surface simulations of this type were recently reported for GeTe(111).[42] Among the key findings is the fact that the surfaces prefer termination by densely packed Te layers throughout; by contrast, the Ge-terminated GeTe(111) surface is least favorable amongst its competitors. For more ionic rocksalt-type structures, the preference for a dense (111) surface is highly unusual, and the best example is rocksalt itself: pristine, that is, dense NaCl(111) surfaces could only in 2000 be realized with considerable effort, while until then only reconstructed

NaCl(111) surfaces had been known.[43] The less polar GeTe seems distinctly different in this regard.

Experimentally, GeTe(111) surfaces have been studied by Yashina et al. using X-ray photoelectron spectroscopy (XPS).[44] The authors also investigated surface oxidation, finding that Ge-terminated surfaces get oxidized readily whereas their Te-terminated counterparts appeared more inert; ultimately, however, a mixture of GeO_2 and TeO_2 encrusts the surface. Again, this was later complemented by periodic DFT.[45] Surface oxidation is a significant issue for practical applications because the resulting oxide layers may inhibit the phase-change process;[46] it thus seems rewarding to further explore atomic oxidation and failure processes of nanoscale PCMs. At present, however, let us proceed to the ideal surfaces of the ternary materials.

Cleaving crystals of well-ordered $Ge_2Sb_2Te_5$ should occur between the weakly vdW-bonded layers (cf. Figure 3), very easily so, and indeed the material largely exposes {0001} facets as seen by TEM.[47] Recall that the hexagonal (0001) surfaces correspond in notation to the rocksalt (111) ones. In fact, both may be observed in one and the same sample, by annealing a previously amorphous film at increasing temperatures; the structural transition and increasing ordering was traced by X-ray diffraction[48] and is (qualitatively!) in line with the scheme of Figure 4b.

Atom-resolved STM investigations have been reported for $GeSb_2Te_4(111)$[49] and $Ge_2Sb_2Te_5(111)$.[38] Both revealed densely packed layers at the surface (Figure 5b). Despite the aesthetic appeal and insight afforded by such imaging techniques, they do not readily reveal which atomic species lie exposed at the surface; again, DFT seems useful to complement the measurements. Doing so showed that Te terminations are most favorable (that is, at lowest surface energies) throughout: cleaving Te···Te contacts incurs very little cost; the computed surface energy is on the order of 10 meV $Å^{-2}$ in a dispersion-corrected DFT framework,[50] which numerically corroborates the intuitive assignment of weak "van der Waals" (vdW) type contacts. Furthermore, Te termination is also favored if cutting within the building blocks (for which there are several distinct options in the ternaries, compared to one single Ge and one single Te termination in GeTe). All this is summarized in so-called surface phase diagrams in Figure 5d: there, each possible termination is characterized by a line, and the horizontal axis spans the range of available chemical potentials (environments).[50] The stability trends nicely underline the aforementioned close similarity between the quasibinary compounds and binary GeTe.

2.4. The Amorphous Phases

Quartz glass is a typical amorphous solid: there is no long-range order, but on the atomic scale it consists of well-defined $[SiO_4]$ tetrahedra throughout, just like crystalline silica. This model, proposed by Zachariasen in the 1930s,[51] is now universally accepted. PCMs are once more highly atypical: their local atomic structure in the amorphous state ("zero bits") does differ strongly from the crystalline one, as first seen by Kolobov et al. in extended X-ray absorption fluorescence spectroscopy (EXAFS) experiments.[52] Further exploration revealed that

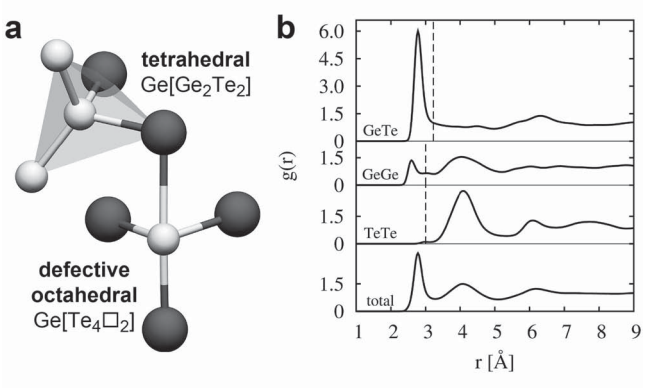

Figure 6. a) Structural fragment from an ab initio MD simulation of amorphous GeTe, drawn as to symbolize the different coordination polyhedra and the occurrence of homopolar (Ge–Ge) bonds in the amorphous phase. Adapted with permission.[53] Copyright 2014, Wiley-VCH Verlag GmbH & Co. KGaA, Weinheim. b) Partial and total pair correlation functions simulated earlier for amorphous GeTe. Dashed vertical lines indicate the cutoff for bonds—which is not trivial to define, because there is no clear minimum beyond the first peak.[53,54] Reprinted figure with permission.[54b] Copyright 2010, American Physical Society.

there is a notable fraction of tetrahedral Ge fragments in the melt-quenched amorphous phases, while no tetrahedra occur in their crystalline counterpart. However, there is no simple model for the amorphous phase but rather the coexistence of several fragments. **Figure 6**a shows a structural motif from a simulation of amorphous GeTe (on which we will elaborate below);[53] there, a tetrahedral entity is indicated which furthermore contains two homopolar Ge–Ge contacts. None of these structural features is found in crystalline GeTe.

As a brief excursion, we may remark that the concept of missing short-range order has been postulated before: Trömel has formulated the idea of "anti-glass", which is disordered in the first coordination shell but exhibits longer-range order; this has been observed in ternary TeO_2-based compounds.[55] PCMs, if one will, thus combine the formal definitions of glass and "anti-glass"; they are neither, and both, because there are still fundamental principles which guide their assembly.

To characterize the structural complexity of amorphous matter, it is customary to condense the entirety of atomic pairs occurring in a given structure into the pair correlation function $g(r)$—or into the partial pair correlation function (PPCF), which runs only over selected contacts. In SiO_2, the first Si–O maximum in the PPCF is very distinct and sharp—these are the covalent bonds, just like in the crystalline phase. Ge–Te bonds, too, exhibit a pronounced peak in the PPCF, at distances around 2.8 Å, but here there is no separation from the longer contacts (Figure 6b); the PPCF drops but stays finite. Note, however, that this plot does not yet give information regarding the angular distribution, that is, the local coordination polyhedra: tetrahedral and octahedral environments will contribute to the same peak in the PPCF if their bond lengths are roughly equal. A look at homopolar contacts is also worthwhile: there are no close Si–Si contacts in quartz glass, but there is a notable amount of short Ge–Ge contacts in amorphous GeTe (as sketched exemplarily in Figure 6a already). Comparable behavior was described for the ternary $Ge_2Sb_2Te_5$.[54a]

Experimentally, the above-shown correlation functions may be obtained by fitting to EXAFS or diffraction experiments. Kolobov's initial studies were followed by others of this type, including investigations into the amorphous structure of AIST.[33a] More key contributions have come from reverse Monte Carlo (RMC) modeling.[56] For a complementary, theoretical investigation of amorphous PCMs, ab initio molecular dynamics (AIMD, or briefly MD in the following) is the method of choice. Initial MD studies dealt with the prototype materials GeTe and $Ge_2Sb_2Te_5$;[54a,57] other compounds from the quasibinary line followed,[58] as did AIST.[33] Results and practical matters of simulations concerned with amorphous PCMs have been aptly reviewed recently,[59] and we will highlight a few key aspects here.

Conventionally, MD models are obtained from a simulated melt-quench procedure, in principle resembling the experimental approach: a simulation cell is loaded with atoms and shaken at very high temperatures (thousands of Kelvin) to randomize the atomic positions; the sample is then equilibrated above the melting point, rapidly quenched, and finally annealed to give an amorphous model.[59] There are major differences, however, between melt-quenched amorphous PCMs and their as-deposited counterparts as they typically result from sputter deposition.[60] For example, the crystallization speed of both can be orders of magnitude different,[61] and so the local atomic order must differ, too. Akola et al. have shown that one can simulate "as deposited" samples, as well: in these simulations, both phases differed strongly in the amount of tetrahedral fragments and homopolar/heteropolar bond distributions.[62] One may assume that a structural contrast of similar nature prevails in "real-world" samples.

The crystallization of PCMs in a typical device proceeds on the order of nanoseconds—which, from an application perspective, is undoubtedly fast. Looking through the eyes of a theorist, much to the contrary, these are very long timescales given that ab initio MD, rather than classical MD is mandatory to capture the complex structural rearrangements during crystallization. Similar discrepancies hold for the system sizes: a simulation box on the length scale of one or two nanometers (thus containing 600–800 atoms) will seem extremely small to the practical physicist, but as of today sets the upper limit of what simulations are capable of.

Very fortunately, there are recent developments that promise to alleviate these limitations, at least to some degree, and thus expand the scope of ab initio MD. For example, it is possible to make simulations significantly faster by merging the seminal Car–Parrinello and Born–Oppenheimer approaches;[63] this is particularly effective when combined with suitably tailored basis sets.[64] Moreover, it was recently shown that a neural-network potential fitted to ab initio energy landscapes[65] can significantly accelerate simulations of the crystallization process while retaining the important physical features. A first neural-network potential has been developed for GeTe[66] and proved capable of describing the transition in large models (≈4000 atoms) and over timescales of several nanoseconds.[67]

Finally, let us stress that the required system sizes depend strongly on the task at hand: local effects call for smaller cells than dynamic processes, and for some questions even the 4000-atom cells may surely not suffice. And in any case, a well-chosen but "cheap" model will outperform a poorly chosen but much larger one.

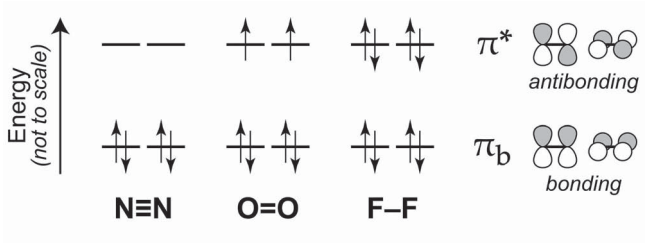

Scheme 1. Simplified schemes for the π frontier orbitals of diatomic N_2, O_2, and F_2, as found in every chemistry textbook. Pictorial representations of the MOs are given, with shading hinting toward the combination coefficients ("in-phase"/"out-of-phase"). The progressive filling of antibonding levels is concomitant with the decrease from a triple, to a double, to a single bond: in F_2, the π MOs do not contribute to the bonding any more, but only a low-lying, filled σ_b orbital (not shown) does.

3. Chemical Bonding in Phase-Change Materials

Solid materials fall into established categories to first approximation: according to their bonding nature, they are labeled as "metallic" (take elemental sodium), "ionic" (rocksalt), or "covalent" (silicon).[28,68] However useful, these terms approach their limits when applied to PCMs—and many other complex solids, for that matter. Over the recent years, bonding has been identified as a key determinant for the properties of phase-change alloys, and great effort has been devoted to unraveling its nature.

The notion of covalent bonding, in particular, is internalized by chemists from the very beginning: they connect atoms by lines (bonds) to form complex entities, and they keep this concept at their heart, largely unimpressed by the fact that Schrödinger's equation does not include any bonds but only electrons and nuclei.[28] Covalent bonding in molecules can be iconized by molecular-orbital (MO) schemes. For example, the progressive filling of the antibonding π^* MOs explains why gaseous N_2, O_2, and F_2 are increasingly easier to dissociate (**Scheme 1**).

The solid-state analogue of such MO schemes is given by eigenvalues in reciprocal space or, after proper integration, by the density-of-states (DOS) plot. Unfortunately, neither band structure nor DOS can be linked to simple pictures as in the molecular case above. We will highlight a possible way out in a moment.

The rigid crystalline networks of diamond and silicon are prototypes of covalently bonded solids. Likewise, covalent bonds prevail in PCMs, as the electronegativity (EN) difference in telluride PCMs is much smaller than in typical ionic crystals ($\Delta EN = 2.2$ in NaCl whereas $\Delta EN = 0.1$ in GeTe).[69] But the situation here is distinctly more complex than in silicon.

3.1. Resonant Bonding

At this point, we must introduce one more of those basic terms, namely, that of resonance. This idea conceived by Pauling[70] originally served to understand the bonding in the benzene (C_6H_6) molecule. Benzene contains six more electrons than would be necessary to form the hexagonal, σ-bonded C_6

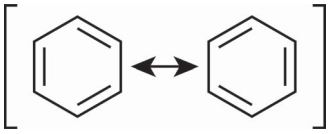

Scheme 2. Sketch of the "resonant" π system in benzene (C_6H_6) as taught in organic chemistry. The correct description of benzene's frontier orbitals is neither that on the left- nor right-hand side alone, but a fully delocalized one.

scaffold. As shown in **Scheme 2**, Pauling proposed a description in terms of degenerate states which are superimposed, that is, in resonance, and together they describe the true nature of the system. Without saying so, we have thereby left the regime of molecular-orbital and stepped into valence-bond (VB) theory.

The concept of resonance has been transferred to the solid state in a seminal work by Lucovsky and White[71] at the example of rocksalt-type IV–VI chalcogenides and elemental selenium and tellurium. Loosely reminiscent of the benzene case, one may view these structures (such as the helical chains in α-Se and α-Te) as containing aligned valence p-orbitals with long-range order, albeit in solids there is usually an undersupply of electrons, contrary to benzene. Such long-range order, and hence "resonant bonding", is absent in the corresponding amorphous phases.[71,72]

Recently, resonant bonding was identified as a characteristic materials fingerprint of PCMs by Shportko et al.,[73] and it leads to a peculiar array of properties. The Born effective charges in the crystalline phase are anomalously large: they reflect the sensitivity of the system toward distortions (which would hamper the orbital alignment and thus the resonance condition). Also, the dielectric constants ε_∞ are high—which is exactly the phenomenon at the origin of the optical contrast, and thus the functional principle of optical disks.[74] We stress at this point that resonance (or aromaticity in molecules) is not trivial to capture by quantum mechanics as a multi-reference wavefunction is at its heart. In other words, resonant bonding cannot be identified by simple MO schemes as shown above, just as the property contrast between crystalline and amorphous PCMs cannot be explained by looking at their electronic DOS, which are quite similar.[75] While a fully quantum-mechanical description of resonant bonding has remained elusive until today, the concept itself has proven no less valuable to understand the very nature of crystalline PCMs. It can even be used as a guideline to search for suitable PCMs (or to rule out unsuitable ones), as will be discussed in Section 5.4 below.

3.2. Peierls Distortions

The term "distortion" is frequently encountered when discussing crystal structures of PCMs. How do such distortions arise? A finger exercise in three dimensions is given by elemental tellurium,[76] whose structure can be derived from a simple cubic lattice by breaking some bonds and strengthening others (**Figure 7**a).[77] Such distortions are caused by instabilities in the electronic structure which, by lowering the crystal symmetry, may be partially removed (concomitant with the opening or increase of a band gap). These mechanisms were

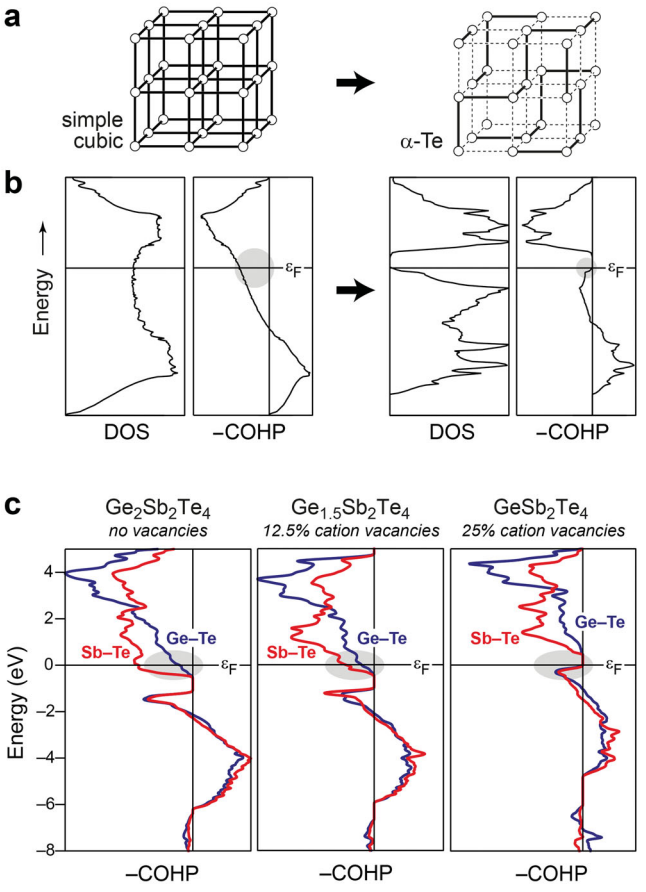

Figure 7. a) Illustration of a Peierls distortion that leads from a simple cubic lattice (left) to the α-Te structure (right).[76,77b] b) Electronic densities of states (DOS) and crystal orbital Hamilton populations (COHP) for both are compared: the Peierls distortion reduces the extent of occupied, antibonding contributions (plotted to the left of the vertical axis and emphasized by shading). Both panels adapted with permission.[76] Copyright 2002, Wiley-VCH Verlag GmbH, Weinheim. c) Chemical bonding in model Ge–Sb–Te alloys as investigated by COHP analysis. Note, again, the reduction of unfavorable interactions near ε_F upon moving from a hypothetical, fully occupied lattice to the "real thing" $GeSb_2Te_4$. Adapted from a previous study.[82]

originally formulated for one-dimensional chains[78] and later extended to the three-dimensional realm.[79] They are now summarily referred to as Peierls distortions.

We reiterate the problem stated above: can one visualize these above-mentioned instabilities in the electronic structure, such as to *see* the driving force for the distortion? More practically, can one retrieve bonding information from the output of a self-consistent computation? The answer is "yes", fortunately, but the precious chemical information is encoded by orbital (or, worse, plane-wave) combination coefficients, usually given on a dense grid in reciprocal space. One must thus extract the local information using suitable tools. Several of the latter have been developed, and we focus on one in the following.

The approach is shown in Figure 7b. For both structures, let us start by inspecting the computed DOS plots. That of the simple cubic lattice has a likewise simple shape, and it

exhibits significant density at the Fermi level, which indicates metallicity. The DOS of the stable α-Te structure shows more distinct features due to the lowered symmetry, and this crystal is predicted to be a semiconductor with a gap at ε_F, correctly so. The bonding inclination may now be visualized by singling out pairs of orbitals at adjacent atoms (that is, off-site contributions to the band structure energy), which leads to a technique dubbed "crystal orbital Hamilton population" (COHP).[80] Like their predecessor, namely, Hughbanks' and Hoffmann's famous "crystal orbital overlap population" (COOP),[81] COHP plots indicate stabilizing interactions on one side of the vertical energy axis, and antibonding ones on the other. The difference between both methods is the criterion used to gauge bonding interactions: overlap in the COOP, expectation values of the Hamiltonian for COHP.[28] The functional principle is comparable otherwise.

We return to the Peierls distortion in elemental Te (Figure 7b). COHP analysis reveals that the interactions around ε_F in the simple cubic structure are indeed antibonding, and significantly so.[83] The distortion, which leads to the stable α-Te structure, largely reduces these unfavorable interactions (gray shading). Likewise, the structure of crystalline GeTe may be rationalized as resulting from a Peierls distortion: compared to the ideal rocksalt lattice, the distortion along [111] lowers the symmetry and stabilizes the overall energetic situation.[84] Distortions are also prevalent in ternary Ge–Sb–Te alloys.[52,85] An interesting question that emerges is why the heavier PbTe, iso(valence)electronic to GeTe, does not show any inclination toward distortion and takes a perfect rocksalt-type lattice. To the best of our knowledge, this question has not yet been answered in full.

3.3. Vacancies and Rigid Bands

The COHP indicator has subsequently been applied to the Ge–Sb–Te system. The first such analysis of GeTe was reported over a decade ago,[86] but not linked to phase-change applications at the time. Subsequently, the method served to explain the reason of the significant vacancy concentrations in a chemical language.[82] To this end, another thought experiment proved useful: starting with the hypothetical rocksalt-type compound $Ge_2Sb_2Te_4$ (with a fully occupied Ge/Sb-containing sublattice), one progressively empties cation sites, until one arrives at the experimentally known rocksalt-type of $GeSb_2Te_4$. For these models and one in between, the computed bond-analytical curves are given in Figure 7c and have been averaged, separately, over the covalent Ge–Te and Sb–Te nearest-neighbor contacts. Moving from left to right, antibonding states (left of the energy axis) are depopulated which stabilizes the remaining crystal. Naturally, each vacancy formed removes six Ge–Te bonds, and thus some antibonding states remain occupied: the overall balance for the crystal's bonding network is presumably most favorable if a compromise is found (between the removal of cations and the strengthening of the remaining bonds). We stress that such behavior is not seen in, say, crystalline silicon: there, all occupied levels are bonding, and all bonding levels are occupied,[80] and forming a single vacancy requires several electronvolts.

With or without saying so, the above argumentation is based on the rigid-band model. The latter is an established concept in the chemistry of intermetallics which served, for example, to rationalize the presence or absence of ferromagnetism in the 3d metals.[87] Subsequently, application of this bond-theoretical concept has enabled the (very practical) design of new magnetic materials.[88] Regarding PCMs, the community is still in the first part of this process—that is, understanding those compounds that are presently being used. But it seems highly rewarding, in the long run, to work toward the second, more predictive part. In other words, it is desirable to find design rules based on microscopic understanding, as previously advocated.[6] For example, it was recently suggested that the control of vacancies but also charge injection (both of which move the Fermi level ε_F, in line with a rigid-band model) can have significant effect on the atomic mobility in defective GeTe.[89]

3.4. Onward to the Amorphous State

The bonding nature of amorphous PCMs can also be investigated with the aforementioned orbital-based tools. At this point, however, a brief technical diversion is necessary. Tools such as COOP and COHP elucidate the interaction of atom-centered orbitals and thus, naturally, have been implemented in the framework of semiempirical and ab initio codes which all rely on local-orbital basis sets. In the 21st century, by stark contrast, simulations of condensed matter often employ modern plane-wave based procedures.[90] The latter basis sets are highly efficient to handle, give precise results, and are inherently well-suited for periodic systems, but they lack the "local" language chemists are accustomed to. Re-extracting local information from plane-wave based simulations would seem most valuable: this topic had been explored in the 1990s already and recently received much attention.[91] Indeed, it has also been possible to regain the quantities shown here from modern plane-wave DFT output, leading to the "projected COHP" (pCOHP)[91c] and similar tools. The implementation within an analytic framework has subsequently been described.[92] Such projection schemes are especially useful whenever "traditional", venerable codes approach their limits and plane-wave techniques take their place: that is, for the study of complex functional materials, e.g., with regard to bonding at surfaces.[93] Likewise, these analyses are applicable to amorphous structures, at least in principle.[53]

In this context, the so-called "bond-weighted distribution function" (BWDF) was introduced,[53] which combines structural information (in the sense of the well-known pair correlation function) with the local bonding nature. In a way, this is reminiscent of the COOP/COHP idea: take a histogram (of electronic levels or of atomic pairs) and weigh it with a suitable quantity which reveals the bonding proclivity; this way, an additional dimension of information is conveniently visualized. The BWDF has initially been defined using the integrated pCOOP, but in principle any suitable indicator may be used that allows for the interpretation of pairwise contacts.

Figure 8a provides a picture similar to the pair correlations seen before (Figure 6b), but now with the bonding information added. It has been resolved according to two criteria. First,

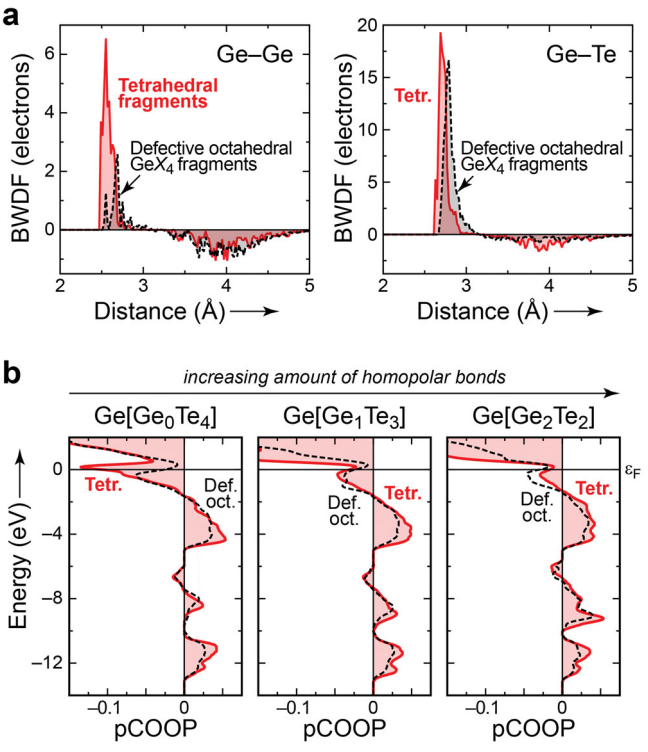

Figure 8. Bonding nature of local structural fragments in amorphous GeTe, as probed by chemical analysis of MD simulation snapshots. a) Bond-weighted distribution functions (BWDF), given separately for homopolar and heteropolar contacts in amorphous GeTe, and also separated according to the local coordination motifs. b) Projected COOP analysis, resolved according to different ligand shells in tetrahedral (red lines) and defective-octahedral (dashed black lines) environments. Reproduced with permission.[53] Copyright 2014, Wiley-VCH Verlag GmbH & Co. KGaA, Weinheim.

homopolar (Ge–Ge) and heteropolar (Ge–Te) bonds are looked at separately; the latter are more abundant, and hence their absolute BWDF values are larger, too. In both cases, the BWDF exhibits a clear-cut maximum at close distances, concomitant with the notion of covalent bonds; Ge–Ge bonds are slightly shorter than Ge–Te ones, unsurprisingly.

A very interesting result is obtained when further dividing the contacts according to local environments (cf. Figure 6a). We emphasize that when discussing structural fragments in PCMs, terms such as "tetrahedra" and "octahedra" are merely approximations, since the polyhedra are strongly distorted (again, other than in the Zachariasen picture). In fact, they can only be classified according to a numerical order parameter,[94] as Caravati et al. have noted.[54a] The Ge–Te contacts, as seen on the right-hand side, are quite insensitive to the coordination environment albeit the bonds in tetrahedra are slightly shorter. Ge–Ge bonds, however, are distinctly less favorable in defective octahedral fragments.

Further studies of this type may now follow two avenues. First, it seems interesting to move from the binary GeTe to ternary alloys such as $Ge_2Sb_2Te_5$ or, even more complex, to AIST: what role do the dopant atoms play in terms of chemical bonding? Second, we have stressed in the preceding section that not all amorphous PCMs are equal: as-deposited samples differ from melt-quenched ones, and all are prone to aging, that is, structural relaxation over time which leads to the dreaded "resistance drift" phenomenon.[95] It would now be most interesting to probe these microscopic subtleties with bond-analytical tools.

4. Charge and Heat Transport

In this section, we briefly touch upon the transport properties of crystalline PCMs, that is, their conduction of heat and electricity. Again, it will become obvious that these materials are puzzling in the best sense.

4.1. Low Heat Conduction in Crystalline PCMs

Traditionally, crystalline materials exhibit good heat conduction, or at least significantly better than their amorphous counterparts (Table 1). Exemplarily, we cite values of 156 ± 8 W m^{-1} K^{-1} for crystalline Si, and 2.6 ± 0.4 W m^{-1} K^{-1} for its amorphous counterpart (measured at 300 K and 293 K, respectively).[96] On the contrary, the heat conduction in crystalline PCMs is remarkably low, and there is often no more than a factor of two between the two phases[97] Microscopically, this behavior has been associated with unusually large atomic displacements in crystalline PCMs, indicating shallow potential-energy landscapes, and with a shift of the phonon spectra to lower frequencies ("softening") upon crystallization.[8] Furthermore, the atomic and vacancy disorder mentioned in Section 2.2 was recently connected to the low heat conductivity, because defects disturb the heat conduction in the crystal (or, in other words, localize the associated phonons).[98] The degree of disorder and thus the thermal conductivity can be tuned by varying the composition, the annealing temperature, or both;[98] see below. Very recently, the low thermal conductivity of crystalline IV–VI compounds has been linked to resonance bonding as reflected, in particular, in long-range dynamic interactions exceeding the first few coordination shells.[99] Further, combined experimental and theoretical investigations of lattice dynamics and bonding now seem rewarding.

4.2. Electrical Transport

The fundamental building blocks of modern electronics are constructed from *p*-type (hole) and n-type (electron) doped semiconductors: think of "pnp" and "npn" transistors. Intriguingly, all PCMs described in the above sections are p-type conducting exclusively, and very significantly so, with hole concentrations on the order of several 10^{20} cm^{-3}.[100] Furthermore, these holes are not generated by extrinsic doping (e.g., trace amounts of Ga atoms doped into crystalline Si) but by a mechanism sometimes referred to as "self-doping". PCMs create charge carriers without any external (chemical) manipulation. Their p-type conductivity is caused by cation vacancies which form in significant amounts beyond those required by stoichiometry. For example, rocksalt-type $GeSb_2Te_4$ exhibits one-quarter of empty lattice sites due to the composition (controlled by the

chemical bonding) alone. At this point, the band corresponds to a textbook semiconductor, with the valence band completely filled (cf. Figure 7c). Removing additional Ge or Sb atoms then leads to p-type conduction by lowering the Fermi level into the valence band. This behavior has been rationalized by careful DFT simulations of defects in GeTe[101] and, later, in $Ge_2Sb_2Te_5$.[102] Figure 7c also qualitatively answers the question why this material class does not exhibit n-type doping: the latter would require the Fermi level to move upward, thereby populating strongly antibonding regions of the band structure.

4.3. Disorder-Induced Localization

To characterize a candidate PCM, one will perform a switching experiment according to the following recipe: deposit an amorphous sample, heat it progressively until the phase transition occurs, then cool down the crystallized material, and measure the electrical resistance during the entire process. The results of such experiments for $GeSb_2Te_4$ are comprised in **Figure 9**.[103] The first part (the crystallization itself) does not look spectacular: the resistance of the initially insulating, amorphous phase decreases while heating, and drops rapidly once the cubic phase (red) is attained. On cooling, however, Siegrist et al. observed a peculiar behavior. The final resistance value differed over several orders of magnitude, depending on the annealing temperature chosen. In addition, the slope of the *R*–*T* curve changed, which indicates a metal–insulator transition (MIT). While MITs are well-known in solid-state physics, they are usually induced by modifying the composition, such as increasing dopant concentration. Here, by contrast, one and the same material is annealed at different temperatures, which fundamentally alters the properties of the phase obtained.[103] Yes, there are formally

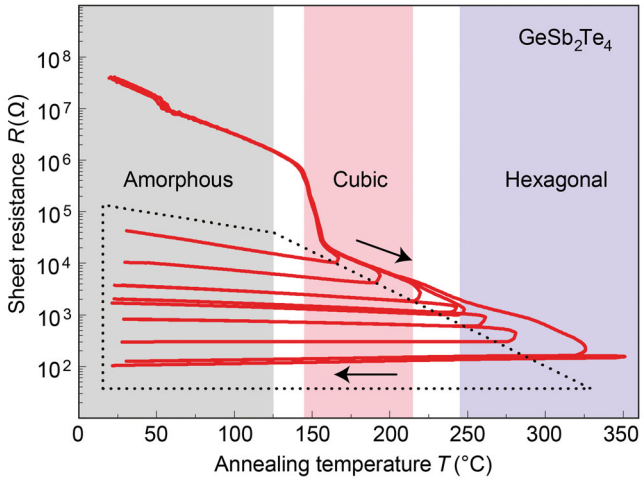

Figure 9. Electrical properties of $GeSb_2Te_4$ films during heating–cooling cycles (arrows): the crystallization is accompanied by a sudden drop in sheet resistance. The final (room-temperature) resistance values of crystallized $GeSb_2Te_4$ span several orders of magnitude, depending on the annealing temperature which may result either in cubic or in (pseudo) hexagonal modifications. Note the change in slopes (negative vs positive) in the region encased by a dotted line, indicating a metal–insulator transition.[103]

two types of crystal structures, metastable (rocksalt-type) and stable ones, but this does not suffice to explain the most diverse behavior observed in Figure 9. Alternatively expressed, we are not dealing with true physicochemical state functions here because the system's behavior does depend on its history in the style of non-equilibrium thermodynamics.

What is the origin of these peculiar effects? The DOS for an arbitrary semiconductor is sketched in **Figure 10**a. The mobility of electrons is controlled by three determinants. The first is the so-called mobility edge, E_μ (black line), which arises from disorder phenomena. The second is the correlation edge, E_C (blue line), but the latter is not influential in PCMs due to their large dielectric constants, which screen the electron–electron interactions (hence $E_\mu \ll E_C$).[103] Finally, the red line shows the location of the Fermi energy E_F which would be changed by tuning the composition or by extrinsic doping; here, however, the same chemical composition is employed and thus E_F is constant in all three panels of Figure 10a. Disorder is hence the decisive determinant in crystalline PCMs: if large enough, it will cause the Fermi level to reside in the localized area, and thus immobilize the valence electrons. This is what happens in rocksalt-type $GeSb_2Te_4$.[103]

To elucidate the atomistic origins of this observation, simulations were subsequently employed.[104] The idea is as follows: construct large models and tune the composition of the cationic sublattice, going from clustered vacancies to perfectly distributed ones (and hence from rocksalt-type to layered models), which qualitatively harmonizes well with the experimental findings of progressive vacancy ordering in related compounds (cf. Figure 4). And indeed, the contrast between localization and delocalization in the highest occupied crystal orbitals (i.e., in the bands near E_F) can be seen by visual inspection of Figure 10b and also by more quantitative numerical indicators which gauge the degree of delocalization.[104] We stress that the model sizes required for such endeavors (thousands of atoms) have been simply unavailable for ab initio computations until a few years ago.

Experimentally, evidence has very recently been provided for an MIT in GeTe nanowires, prior to amorphization, and it has been attributed to increased disorder.[105] Intriguingly, this MIT is due to a different microscopic mechanism, having been induced by stacking faults and thus two-dimensionally extended defects. In both cases, however, the composition of the sample (thus E_F) remains unchanged, and the MIT is controlled by influencing the mobility edge E_μ alone. The crucial role of stacking faults for the fast switching in nanowires has been demonstrated by experiment and simulation before.[106] All this highlights the fascinating complexity of PCMs, and of their defect nature: there is more than one single atomic mechanism, and different approaches may, and do, independently lead to success.

5. Strategies for New and Improved Materials

$Ge_2Sb_2Te_5$ and its chemical relatives are widely used by industry, which might create the impression that optimal materials have already been found. In stark contrast, there is still much room, and a clear need, to find PCMs with improved properties—for example, with better high-temperature stability.

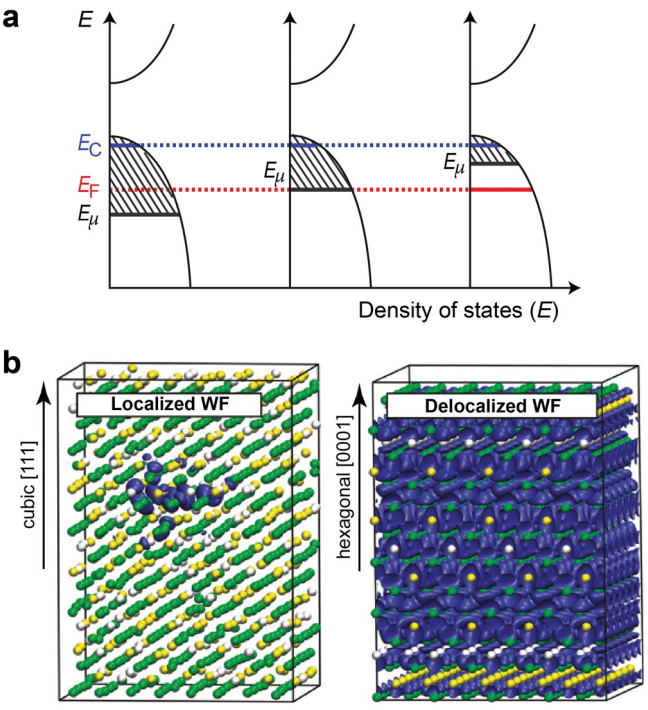

Figure 10. a) Simplified band scheme for crystalline *p*-type materials such as $GeSb_2Te_4$. The region above the mobility edge E_μ has been shaded and leads to insulating behavior if the Fermi level E_F resides there. From.[103] b) Localization of the highest occupied crystal orbital in large models of crystalline $GeSb_2Te_4$, either with fully randomly distributed vacancies (left) to fully ordered layers (right). From a previous study.[104]

Here, we outline two major strategies that have been followed toward such goal. First, one can fabricate more complex, precisely controlled structures, such as nanowires or superlattices, and thereby add exciting new aspects to "known" compounds such as $Ge_2Sb_2Te_5$. Second, it seems desirable to find wholly new PCMs with desirable microscopic properties.

5.1. Nanoparticles

There are several routes for synthesizing nanostructures, and two are regularly followed to create nanoscale PCMs. One is the vapor–liquid–solid (VLS) technique which typically employs gold nanoparticles as catalysts.[37,107] For example, this led to nanowires as already shown in Figure 5a, and the study of these very specimens revealed significantly lower power consumption than required to switch bulk PCMs.[37] The second option is a "traditionally" chemical one: namely, synthesis from the liquid phase (and with suitable ligands), which has been mainly explored for GeTe nanostructures so far.[39,108] The latter approach, for example, allowed for the discovery of polarization domains in nanoscale GeTe[108c] and for detailed investigations of amorphous particles.[108d] In such syntheses, the influence of surfactants and, more colloquially, "dirt" in the reaction mixture is crucial, as has been outlined in an interesting essay by Hoffmann.[109] Synthesis and scaling trends of PCM nanoparticles have recently been reviewed at greater length than is possible here.[110]

5.2. Superlattices and Interfacial Phase-Change Memory

A look back at Figure 3 shows well-ordered, idealized structures of telluride materials, iconized in terms of different building blocks which are then stacked along [0001]. But the situation is less ideal in reality, where significant degrees of disorder are present (Section 2); this is even more relevant for samples which are not grown under laboratory conditions but constitute as-crystallized bits in an actual device. It would now seem advantageous to gain more precise control of the atomic ordering in PCMs. With new advances in epitaxial growth, one may indeed proceed from the "traditional" layered materials to more precisely ordered superlattice-like structures.[111]

Building thereupon, Simpson et al. introduced the "interfacial phase-change memory" (iPCM),[112] that is, a precisely ordered stack of different structural building blocks, grown by use of a physical vapor deposition system. It was found that the energy requirement of such iPCM is nearly an order of magnitude lower than for conventional $Ge_2Sb_2Te_5$ cells[112]—a most significant gain. The precise switching mechanisms, however, are far from fully understood and lay out rewarding targets for future work.

A (truly) ancient notion divides chemistry into two disciplines: analysis and synthesis. The idea of "building blocks" can be taken further in this classical language: after analyzing the structure based on careful diffraction experiments, one may proceed to construct, to "synthesize", if one will, more complex frameworks. For example, earlier work proposed a superlattice-like combination of GeTe and Sb_7Te_3,[113] and thus a combination of two structural families that have been discussed in Section 2. More recently, a mechanism was suggested that involves GeTe bilayers "sandwiched" between Sb_2Te_3 building blocks,[114] continuing the line of thought regarding iPCM. Again, tried-and-true concepts merge with new techniques here: it has been noted decades ago that GeTe is the simplest known ferroelectric,[115] and one can now try to switch ferroelectricity on and off within these bilayers.[114]

5.3. Beyond Ge–Sb–Te

So far, new functionality has been achieved by altering the structural nature or dimensionality of established PCMs, such as the evergreen $Ge_2Sb_2Te_5$. Beyond that, it seems equally desirable to explore different compositions. In fact, these "new" compounds are usually long-known solid-state phases which are now being rediscovered for phase-change applications.

One such example is GaSb, a textbook III–V semiconductor. Gallium–antimony alloys have been probed as possible data-storage alloys a quarter century ago already[116] and recently gained renewed attention: electrical switching[117] and NMR experiments[118] have been performed, as have a number of recent MD simulations.[119] These studies have been concerned with the stoichiometrically precise composition GaSb, but also with more Sb-rich alloys such as $GaSb_7$. It is important to note that there are no Sb-rich gallium–antimony phases in the Inorganic Crystal Structure Database (ICSD). There is thus segregation on the atomic scale, as observed during MD.[119a] Furthermore, the concept of resonance bonding, identified earlier as a

fingerprint of Ge–Sb–Te alloys, cannot be seamlessly expanded to these compounds, even more so as the atomic environments in (zincblende-type) GaSb show tetrahedral coordination throughout and no Peierls distortions. Possibly, new microscopic theories and descriptors will be needed to continue the search for PCMs in this materials class.

Another example is In_3SbTe_2, a metastable quasibinary mixture of InSb and InTe.[120] Again, In_3SbTe_2 is not a "new" PCM, having been discovered already in the late 1980s,[121] but it has likewise been dormant, possibly because the atomic phase-change mechanisms could not be fully resolved at that time. In_3SbTe_2 forms the only entry in the ternary In–Sb–Te system and crystallizes in the rocksalt type (with Sb/Te statistically sharing the anionic sublattice). Neither InSb nor InTe do so in thermodynamic equilibrium. In both aspects, In_3SbTe_2 is thus radically different from the wide range of quasibinary Ge–Sb–Te alloys which are all intimately related to the binaries (Figure 3). There are also differences regarding the occurrence and amount of vacancies: multiple diffraction techniques did not show evidence of vacancies (or significant local distortions, for that matter) in rocksalt-type In_3SbTe_2.[122] Furthermore, experiments suggest that the crystallization of the indium-based alloy proceeds via microstructures which give rise to distinct resistivity changes.[123]

There are intriguing open questions: How do the different crystallization steps ("multibits") look like on an atomic scale; are they phase-pure, and on which length scale? Is it possible to alloy In_3SbTe_2 and $Ge_2Sb_2Te_5$, which both possess rocksalt lattices with rather similar lattice parameters, but very different atomic distributions (that is, mixed occupations on the anionic sublattice for In_3SbTe_2, and on the cationic sublattice for $Ge_2Sb_2Te_5$)?[124] And, finally: is it possible to find a generic fingerprint that is shared by these seemingly different materials?

5.4. New Materials by Design?

The above examples have alluded to a simple (and sad) fact: the space of chemical compositions holds a cornucopia of materials, but only few are truly suitable for practical applications. Fortunately, rather than brute-forcing the answer, chemists and physicists have come up with empirical (and clever) schemes to try and locate those regions of composition space which are most likely to host the desired materials class. The creation of "structure maps" is a classical and recurring theme in condensed-matter theory.[125] Naturally, this story starts with *AB* compounds and their textbook structure types (rocksalt, zincblende, etc.)

In the late 1960s already, Phillips and van Vechten suggested to "map out" solid-state compounds according to their covalent and ionic nature.[125a] The first descriptor is thus linked to hybridization (or orbital mixing) and the second to the electronegativity. For example, in NaCl a concept such as "sp^3" hybridization is close to irrelevant, but the EN difference between Na and Cl is high; on the other hand, silicon is an archetype of "sp^3" systems whereas there is naturally no ionic bonding. Orbital-based (pseudopotential-like) quantities were used for maps by St. John and Bloch,[125b] and work along these lines was significantly expanded in the sequel: empirical schemes served to map out almost 500 AB compounds,[125c] and to understand trends in the physical and chemical properties of IV–VI materials.[125d] We emphasize here the sheer efficiency of such approaches: they required, and require, almost no computational power; structure maps of the above kind can be constructed using a compendium of tabulated values and a pocket calculator. Of course, computational resources and reliable DFT codes are widely available today, but they must not replace physical and chemical understanding.

While the traditional concept of materials mapping was employed to characterize known compounds, more recent work suggested to exploit the predictive quality of such techniques. Hence, a "treasure map" for finding PCMs has been proposed in 2008,[84a] and it is shown in **Figure 11**a. Two coordinates span this map, along the schemes described above: on the horizontal axis, the ionicity is given, which is large in PbO (bottom right) and continuously decreases upon going to PbTe, for example. The vertical axis is arguably even more important: it measures the degree of s–p orbital "hybridization" or mixing and thus the proclivity to form "sp^3"-like networks. PCMs are marked by green dots in the above materials map, and it is evident that they fall in a very small range with low ionicity and low hybridization. As a rule of thumb, tetrahedrally bonded ("sp^3"-like) solids show neither resonant bonding nor phase-change characteristics.[6,127] We stress that the coordinates are thus far based on empirical criteria such as orbital radii. Invariably, the use of atomic quantities cannot capture the structural peculiarities of multinary phases, especially when polymorphism is involved. Further work in our laboratories is concerned with ab initio derived coordinates to capture the materials' subtleties even better.

In itself already, the de novo search for PCMs seems a rewarding goal. Recently, it has been proposed to take this search scheme one step further and to extend it to other classes of functional materials.[126] Figure 11b shows a revised version of the above-mentioned map, spanned by the same coordinates but now highlighting other applications, too. It is striking that these very different functionalities seem to occur in closely neighboring (and often identical) compounds.

Finally, it seems tempting to reverse the above argumentation. Figure 11b suggested that other families of functional materials are found close to PCMs on the structure map. Is it possible, in turn, to use PCMs for entirely different applications?

6. New Applications

We round out this work by highlighting new applications of PCMs beyond the widely established ones. However diverse, they share the common ground of making creative use of the materials' property portfolio. Some of these applications are very young, merely at the proof-of-concept stage, but nonetheless they serve as inspiring representatives of what this class of materials has to offer.

For example, optical media such as the re-writeable Blu-Ray disk are widely used in industry,[3c] but there are more ideas for exploiting the optical properties of PCMs. The use in optoelectronic devices has been demonstrated recently: one can induce

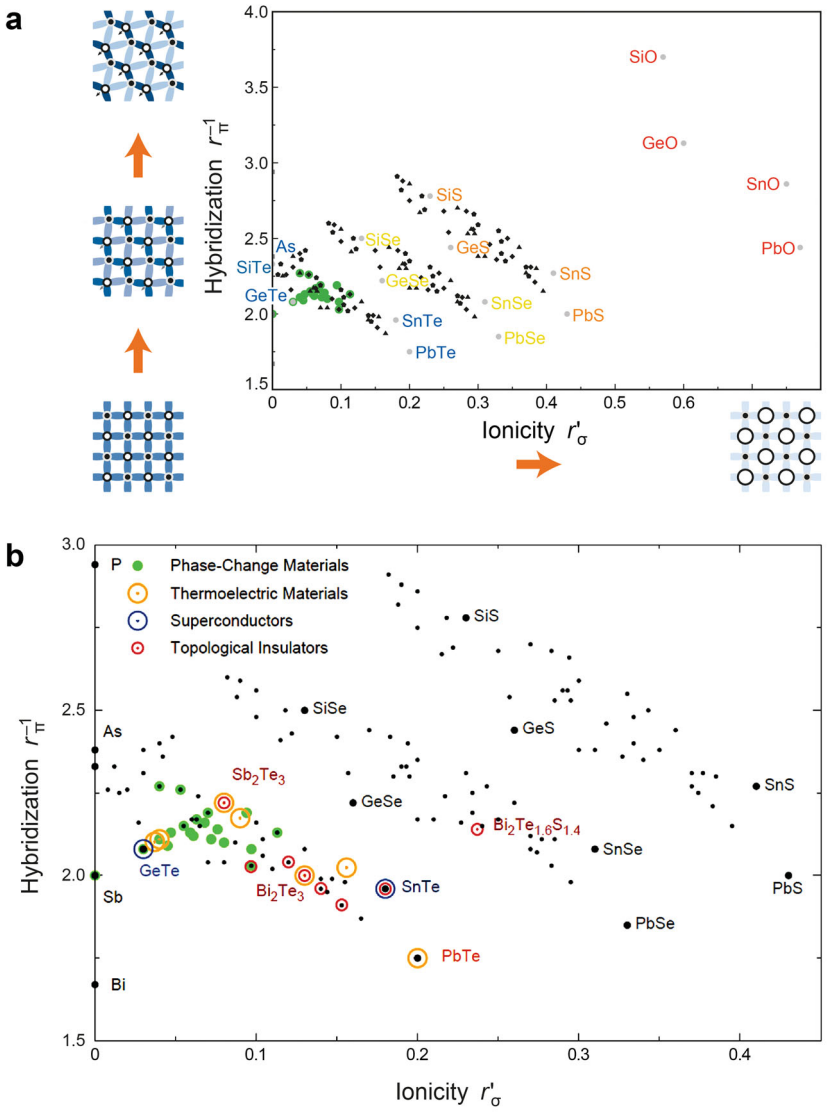

Figure 11. Structure maps for elements and alloys with an average *p*-electron count of three in the valence. a) The first "map for PCMs" as described in the text; suitable compositions are highlighted by green bullets and found to cluster in the lower left region of the map. From Ref. [84a]. b) Extended "treasure map" which includes additional compounds and, importantly, different functionalities. This underlines the versatile property portfolio of telluride materials, and evidences that one can locate such compounds on a materials map. Reproduced with permission.[126] Copyright 2012, Wiley-VCH Verlag GmbH & Co. KGaA, Weinheim.

color changes in $Ge_2Sb_2Te_5$ layers deposited on substrate films of different thickness, which can be rapidly switched (and much more rapidly so than flat-screen panels and other current display technology); in the long run, this could provide engineers with new ingredients for flexible displays, "smart paper" and the like.[128] Furthermore, PCMs are increasingly employed in plasmonic devices, for tuning the resonance of antennae, and for other optical applications.[129]

Another interesting link comes from the electronic structure. We have discussed Sb_2Te_3 here as a parent compound of PCMs, but by far most attention currently devoted to it stems from the fact that Sb_2Te_3 was found to be a topological insulator (TI).[130] TIs are an emerging class of functional materials with prospective applications such as in quantum computers.[131] Based on DFT computations, TI properties of layered $Ge_2Sb_2Te_5$ have been predicted for one of the ideal stacking sequences but not for another.[132] Also, the possibility of inducing the TI phase by external force, such as strain, has been discussed.[133] However, the role of the layer stacking and cation ordering remains to be verified (if one stacking sequence leads to TI properties and the other does not, what happens for mixed occupations?). The inherent disorder in the ternaries is naturally much higher than in Sb_2Te_3; on the other hand, the above-mentioned advances in epitaxial growth may prove extremely valuable with regard to TIs, too. Recently, ARPES measurements on $Ge_2Sb_2Te_5$ have been performed to probe the topological nature of the surface bands.[38] Investigations in this direction are still ongoing.

The surprisingly low thermal conductivity of PCMs was highlighted above, as well. This property makes them principally interesting for use in thermoelectrics, as various groups have noted recently.[134] Thermoelectric devices turn heat into electricity and thus find broad application in power generation from waste heat, or for Peltier-style cooling.[135] As one example, crystallized Ge-rich tellurides, reminiscent of what was shown in Figure 4, have been investigated for this purpose.[34b] The recently established link between resonant bonding and low thermal conductivity connects both fields more intimately:[99] the search for new thermoelectrics, likewise, may target resonantly bonded solids. In this light, we reiterate that both aforementioned classes of materials, topological insulators and thermoelectrics, are found near PCMs on the extended "treasure map" of Figure 11b.

The final aspect concerns the processing of information. Even today's most advanced supercomputers pale before natural "computing systems"—that is, before the brain, which is not only significantly more powerful but also more energy-efficient by several orders of magnitude. There are fundamental differences between the functionality of today's computer architecture ("von Neumann" type logic) and that of neuronal systems. Ovshinsky, the father of phase-change technology, suggested that one might use such materials for neuromorphic computing.[136] And indeed it was recently demonstrated that accumulation (switching after a certain number of pulses, thereby mimicking a biological synapse) is possible using PCMs, and successful prototypes have been reported.[137]

As said above, many applications that we have touched upon here are at a very early stage. Maybe some will remain concepts, but maybe others will become extremely important

in the future. No matter what, they illustrate a key message that we have tried to convey: the phase-change community has very powerful compounds in their hands which, given creativity and flexibility, will continue to provide a useful materials platform for most diverse applications. The investigation of fundamental, microscopic properties is rarely a "flashy" or a fashionable task, but a very necessary one: then, and only then, will one be able to put the carefully accumulated knowledge to use, and to create new materials with desirable properties. We believe that the most exciting discoveries in this regard lie yet ahead.

Acknowledgements

The authors thank the Deutsche Forschungsgemeinschaft (DFG) for generously supporting their studies in the framework of SFB 917 "Nanoswitches". M.W. is funded by the European Research Council (ERC) through an ERC Advanced Grant.

Received: February 2, 2015
Revised: April 28, 2015
Published online: June 10, 2015

[1] S. R. Ovshinsky, *Phys. Rev. Lett.* **1968**, *21*, 1450.
[2] M. Wuttig, N. Yamada, *Nat. Mater.* **2007**, *6*, 824.
[3] a) N. Yamada, E. Ohno, N. Akahira, K. Nishiuchi, K. Nagata, M. Takao, *Jpn. J. Appl. Phys., Suppl. 26–4* **1987**, *26*, 61; b) N. Yamada, E. Ohno, K. Nishiuchi, N. Akahira, M. Takao, *J. Appl. Phys.* **1991**, *69*, 2849; c) N. Yamada, *Phys. Status Solidi (b)* **2012**, *249*, 1837.
[4] a) M. H. R. Lankhorst, B. W. S. M. M. Ketelaars, R. A. M. Wolters, *Nat. Mater.* **2005**, *4*, 347; b) M. Wuttig, *Nat. Mater.* **2005**, *4*, 265; c) G. Atwood, *Science* **2008**, *321*, 210.
[5] S. Raoux, M. Wuttig, *Phase Change Materials: Science and Applications*, Springer, New York **2009**.
[6] D. Lencer, M. Salinga, M. Wuttig, *Adv. Mater.* **2011**, *23*, 2030.
[7] D. C. Hyun, N. S. Levinson, U. Jeong, Y. Xia, *Angew. Chem. Int. Ed.* **2014**, *53*, 3780.
[8] T. Matsunaga, N. Yamada, R. Kojima, S. Shamoto, M. Sato, H. Tanida, T. Uruga, S. Kohara, M. Takata, P. Zalden, G. Bruns, I. Sergueev, H. C. Wille, R. P. Hermann, M. Wuttig, *Adv. Funct. Mater.* **2011**, *21*, 2232.
[9] D. Ielmini, A. L. Lacaita, *Mater. Today* **2011**, *14*, 600.
[10] G. W. Burr, M. J. Breitwisch, M. Franceschini, D. Garetto, K. Gopalakrishnan, B. Jackson, B. Kurdi, C. Lam, L. A. Lastras, A. Padilla, B. Rajendran, S. Raoux, R. S. Shenoy, *J. Vac. Sci. Technol. B* **2010**, *28*, 223.
[11] A. V. Kolobov, J. Tominaga, *Chalcogenides: Metastability and Phase Change Phenomena*, Springer, Heidelberg, New York **2012**.
[12] G. Bruns, P. Merkelbach, C. Schlockermann, M. Salinga, M. Wuttig, T. D. Happ, J. B. Philipp, M. Kund, *Appl. Phys. Lett.* **2009**, *95*, 043108.
[13] W. Klemm, G. Frischmuth, *Z. Anorg. Allg. Chem.* **1934**, *218*, 249.
[14] K. Schubert, H. Fricke, *Z. Naturforsch.* **1951**, *6a*, 781.
[15] J. Goldak, C. S. Barrett, D. Innes, W. Youdelis, *J. Chem. Phys.* **1966**, *44*, 3323.
[16] T. Chattopadhyay, J. X. Boucherle, H. G. von Schnering, *J. Phys. C: Solid State Phys.* **1987**, *20*, 1431.
[17] V. L. Deringer, *Dissertation*, RWTH Aachen University, Germany **2014**.
[18] R. B. Sosman, *The phases of silica*, Rutgers University Press, New Brunswick, NJ, **1965**.
[19] a) P. Fons, A. V. Kolobov, M. Krbal, J. Tominaga, K. S. Andrikopoulos, S. N. Yannopoulos, G. A. Voyiatzis, T. Uruga, *Phys. Rev. B* **2010**, *82*, 155209; b) T. Matsunaga, P. Fons, A. V. Kolobov, J. Tominaga, N. Yamada, *Appl. Phys. Lett.* **2011**, *99*, 231907; c) M. Krbal, A. V. Kolobov, P. Fons, J. Tominaga, S. R. Elliott, J. Hegedus, A. Giussani, K. Perumal, R. Calarco, T. Matsunaga, N. Yamada, K. Nitta, T. Uruga, *Phys. Rev. B* **2012**, *86*, 045212.
[20] U. D. Wdowik, K. Parlinski, S. Rols, T. Chatterji, *Phys. Rev. B* **2014**, *89*, 224306.
[21] S. A. Semiletov, *Sov. Phys. Crystallogr.* **1956**, *1*, 317.
[22] J. L. F. Da Silva, A. Walsh, H. Lee, *Phys. Rev. B* **2008**, *78*, 224111.
[23] K. Momma, F. Izumi, *J. Appl. Cryst.* **2011**, *44*, 1272.
[24] M. N. Schneider, M. Seibald, P. Lagally, O. Oeckler, *J. Appl. Cryst.* **2010**, *43*, 1012.
[25] I. I. Petrov, R. M. Imamov, Z. G. Pinsker, *Sov. Phys. Crystallogr.* **1968**, *13*, 339.
[26] B. J. Kooi, J. T. M. De Hosson, *J. Appl. Phys.* **2002**, *92*, 3584.
[27] a) $GeSb_2Te_4$: T. Matsunaga, N. Yamada, *Phys. Rev. B* **2004**, *69*, 104111; b) $Ge_2Sb_2Te_5$: T. Matsunaga, N. Yamada, Y. Kubota, *Acta Crystallogr., Sect. B* **2004**, *60*, 685; c) $Ge_8Sb_2Te_{11}$: T. Matsunaga, H. Morita, R. Kojima, N. Yamada, K. Kifune, Y. Kubota, Y. Tabata, J.-J. Kim, M. Kobata, E. Ikenaga, K. Kobayashi, *J. Appl. Phys.* **2008**, *103*, 093511.
[28] R. Dronskowski, *Computational Chemistry of Solid State Materials*, Wiley-VCH, Weinheim **2005**.
[29] Z. M. Sun, J. Zhou, R. Ahuja, *Phys. Rev. Lett.* **2006**, *96*, 055507.
[30] H. Iwasaki, Y. Ide, M. Harigaya, Y. Kageyama, I. Fujimura, *Jpn. J. Appl. Phys., Part 1* **1992**, *31*, 461.
[31] V. Agafonov, N. Rodier, R. Céolin, R. Bellissent, C. Bergman, J. P. Gaspard, *Acta Crystallogr., Sect. C* **1991**, *47*, 1141.
[32] K. Kifune, Y. Kubota, T. Matsunaga, N. Yamada, *Acta Crystallogr., Sect. B* **2005**, *61*, 492.
[33] a) T. Matsunaga, J. Akola, S. Kohara, T. Honma, K. Kobayashi, E. Ikenaga, R. O. Jones, N. Yamada, M. Takata, R. Kojima, *Nat. Mater.* **2011**, *10*, 129; b) W. Zhang, I. Ronneberger, P. Zalden, M. Xu, M. Salinga, M. Wuttig, R. Mazzarello, *Sci. Rep.* **2014**, *4*, 6529.
[34] a) M. N. Schneider, P. Urban, A. Leineweber, M. Döblinger, O. Oeckler, *Phys. Rev. B* **2010**, *81*, 184102; b) T. Rosenthal, M. N. Schneider, C. Stiewe, M. Döblinger, O. Oeckler, *Chem. Mater.* **2011**, *23*, 4349; c) M. N. Schneider, X. Biquard, C. Stiewe, T. Schröder, P. Urban, O. Oeckler, *Chem. Commun.* **2012**, *48*, 2192.
[35] a) S. Raoux, J. L. Jordan-Sweet, A. J. Kellock, *J. Appl. Phys.* **2008**, *103*, 114310; b) R. E. Simpson, M. Krbal, P. Fons, A. V. Kolobov, J. Tominaga, T. Uruga, H. Tanida, *Nano Lett.* **2010**, *10*, 414.
[36] a) K. L. Chopra, S. K. Bahl, *J. Appl. Phys.* **1969**, *40*, 4171; b) S. K. Bahl, K. L. Chopra, *J. Appl. Phys.* **1969**, *40*, 4940; c) S. K. Bahl, K. L. Chopra, *J. Appl. Phys.* **1970**, *41*, 2196.
[37] S.-H. Lee, Y. Jung, R. Agarwal, *Nat. Nanotechnol.* **2007**, *2*, 626.
[38] C. Pauly, M. Liebmann, A. Giussani, J. Kellner, S. Just, J. Sánchez-Barriga, E. Rienks, O. Rader, R. Calarco, G. Bihlmayer, M. Morgenstern, *Appl. Phys. Lett.* **2013**, *103*, 243109.
[39] S. Schulz, S. Heimann, K. Kaiser, O. Prymak, W. Assenmacher, J. T. Brüggemann, B. Mallick, A.-V. Mudring, *Inorg. Chem.* **2013**, *52*, 14326.
[40] L. V. Yashina, R. Püttner, V. S. Neudachina, T. S. Zyubina, V. I. Shtanov, M. V. Poygin, *J. Appl. Phys.* **2008**, *103*, 094909.
[41] A. Groß, *Theoretical Surface Science: A Microscopic Perspective*, Springer, Berlin, Heidelberg, New York **2009**.
[42] V. L. Deringer, M. Lumeij, R. Dronskowski, *J. Phys. Chem. C* **2012**, *116*, 15801.

[43] W. Hebenstreit, M. Schmid, J. Redinger, R. Podloucky, P. Varga, *Phys. Rev. Lett.* **2000**, *85*, 5376.
[44] L. V. Yashina, R. Püttner, V. S. Neudachina, T. S. Zyubina, V. I. Shtanov, M. V. Poygin, *J. Appl. Phys.* **2008**, *103*, 094909.
[45] V. L. Deringer, R. Dronskowski, *J. Appl. Phys.* **2014**, *116*, 173703.
[46] E. Gourvest, B. Pelissier, C. Vallée, A. Roule, S. Lhostis, S. Maitrejean, *J. Electrochem. Soc.* **2012**, *159*, H373.
[47] Y. J. Park, J. Y. Lee, Y. T. Kim, *Appl. Phys. Lett.* **2006**, *88*, 201905.
[48] V. Bragaglia, B. Jenichen, A. Giussani, K. Perumal, H. Riechert, R. Calarco, *J. Appl. Phys.* **2014**, 054913.
[49] D. Subramaniam, C. Pauly, M. Liebmann, M. Woda, P. Rausch, P. Merkelbach, M. Wuttig, M. Morgenstern, *Appl. Phys. Lett.* **2009**, *95*, 103110.
[50] V. L. Deringer, R. Dronskowski, *J. Phys. Chem. C* **2013**, *117*, 15075.
[51] W. Zachariasen, *J. Am. Chem. Soc.* **1932**, *54*, 3841.
[52] A. V. Kolobov, P. Fons, A. I. Frenkel, A. L. Ankudinov, J. Tominaga, T. Uruga, *Nat. Mater.* **2004**, *3*, 703.
[53] V. L. Deringer, W. Zhang, M. Lumeij, S. Maintz, M. Wuttig, R. Mazzarello, R. Dronskowski, *Angew. Chem. Int. Ed.* **2014**, *53*, 10817.
[54] a) S. Caravati, M. Bernasconi, T. D. Kühne, M. Krack, M. Parrinello, *Appl. Phys. Lett.* **2007**, *91*, 171906; b) R. Mazzarello, S. Caravati, S. Angioletti-Uberti, M. Bernasconi, M. Parrinello, *Phys. Rev. Lett.* **2010**, *104*, 085503.
[55] M. Trömel, *Z. Kristallogr.* **1988**, *183*, 15.
[56] K. Ohara, L. Temleitner, K. Sugimoto, S. Kohara, T. Matsunaga, L. Pusztai, M. Itou, H. Ohsumi, R. Kojima, N. Yamada, T. Usuki, A. Fujiwara, M. Takata, *Adv. Funct. Mater.* **2012**, *22*, 2251.
[57] a) J. Akola, R. O. Jones, *Phys. Rev. B* **2007**, *76*, 235201; b) J. Hegedüs, S. R. Elliott, *Nat. Mater.* **2008**, *7*, 399.
[58] a) J. Akola, R. O. Jones, *Phys. Rev. B* **2009**, *79*, 134118; b) S. Caravati, M. Bernasconi, M. Parrinello, *Phys. Rev. B* **2010**, *81*, 014201.
[59] J. Akola, R. O. Jones, *Phys. Status Solidi (b)* **2012**, *249*, 1851.
[60] J. H. Coombs, A. P. J. M. Jongenelis, W. van Es-Spiekman, B. A. J. Jacobs, *J. Appl. Phys.* **1995**, *78*, 4906.
[61] a) J. Orava, A. L. Greer, B. Gholipour, D. W. Hewak, C. E. Smith, *Nat. Mater.* **2012**, *11*, 279; b) M. Salinga, E. Carria, A. Kaldenbach, M. Bornhöfft, J. Benke, J. Mayer, M. Wuttig, *Nat. Commun.* **2013**, *4*, 2371; c) Without going into detail here, the crystallization speed can be further improved by structural pre-ordering, that is, again by atomic-scale complexity: D. Loke, T. H. Lee, W. J. Wang, L. P. Shi, R. Zhao, Y. C. Yeo, T. C. Chong, S. R. Elliott, *Science* **2012**, *336*, 1566.
[62] J. Akola, J. Larrucea, R. O. Jones, *Phys. Rev. B* **2011**, *83*, 094113.
[63] T. D. Kühne, M. Krack, F. R. Mohamed, M. Parrinello, *Phys. Rev. Lett.* **2007**, *98*, 066401.
[64] J. Van de Vondele, M. Krack, F. Mohamed, M. Parrinello, T. Chassaing, J. Hutter, *Comput. Phys. Commun.* **2005**, *167*, 103.
[65] J. Behler, *J. Phys.: Condens. Matter* **2014**, *26*, 183001.
[66] G. C. Sosso, G. Miceli, S. Caravati, J. Behler, M. Bernasconi, *Phys. Rev. B* **2012**, *85*, 174103.
[67] G. C. Sosso, G. Miceli, S. Caravati, F. Giberti, J. Behler, M. Bernasconi, *J. Phys. Chem. Lett.* **2013**, *4*, 4241.
[68] Quantum chemistry also teaches that "metallic bonding" is an extreme case of covalency for large particle numbers (atoms) and an undersupply of electrons to share.
[69] L. Pauling, *J. Am. Chem. Soc.* **1932**, *54*, 3570.
[70] L. Pauling, *The Nature of the Chemical Bond*, 3rd ed., Cornell University Press, Ithaca **1960**.
[71] G. Lucovsky, R. M. White, *Phys. Rev. B* **1973**, *8*, 660.
[72] B. Huang, J. Robertson, *Phys. Rev. B* **2010**, *81*, 081204(R).
[73] K. Shportko, S. Kremers, M. Woda, D. Lencer, J. Robertson, M. Wuttig, *Nat. Mater.* **2008**, *7*, 653.
[74] W. Wełnic, S. Botti, L. Reining, M. Wuttig, *Phys. Rev. Lett.* **2007**, *98*, 236403.
[75] N. J. Shevchik, J. Tejeda, D. W. Langer, M. Cardona, *Phys. Rev. Lett.* **1973**, *30*, 659.
[76] A. Decker, G. A. Landrum, R. Dronskowski, *Z. Anorg. Allg. Chem.* **2002**, *628*, 295.
[77] a) We note in passing that several pathways exist for doing so—formally, there are an additional thirty-five thinkable structures that can be derived from the simple cubic lattice. See: J. K. Burdett, T. J. McLarnan, *J. Chem. Phys.* **1981**, *75*, 5764; b) The Peierls-distorted crystal structure of elemental Te has been derived along these lines, previously, in J.-P. Gaspard, A. Pellegatti, F. Marinelli, C. Bichara, *Philos. Mag. B* **1998**, *77*, 727.
[78] R. E. Peierls, *Quantum Theory of Solids*, Oxford University Press, Oxford **1955**.
[79] J. K. Burdett, S. Lee, *J. Am. Chem. Soc.* **1983**, *105*, 1079.
[80] R. Dronskowski, P. E. Blöchl, *J. Phys. Chem.* **1993**, *97*, 8617.
[81] T. Hughbanks, R. Hoffmann, *J. Am. Chem. Soc.* **1983**, *105*, 3528.
[82] M. Wuttig, D. Lüsebrink, D. Wamwangi, W. Wełnic, M. Gilleßen, R. Dronskowski, *Nat. Mater.* **2007**, *6*, 122.
[83] We stress that the mere existence of a finite DOS at the Fermi level does not indicate de-stabilization—otherwise, all metals would be unstable.
[84] a) D. Lencer, M. Salinga, B. Grabowski, T. Hickel, J. Neugebauer, M. Wuttig, *Nat. Mater.* **2008**, *7*, 972; b) Note that the concept of Peierls distortions is not limited to crystalline materials, or even to the solid state at all. Evidence for a Peierls distortion in liquid GeTe has been found in J. Y. Raty, V. Godlevsky, Ph. Ghosez, C. Bichara, J. P. Gaspard, J. R. Chelikowsky, *Phys. Rev. Lett.* **2000**, *85*, 1950.
[85] S. Shamoto, N. Yamada, T. Matsunaga, T. Proffen, J. W. Richardson, J.-H. Chung, T. Egami, *Appl. Phys. Lett.* **2005**, *86*, 081904.
[86] U. V. Waghmare, N. A. Spaldin, H. C. Kandpal, R. Seshadri, *Phys. Rev. B* **2003**, *67*, 125111.
[87] G. A. Landrum, R. Dronskowski, *Angew. Chem. Int. Ed.* **2000**, *39*, 1560.
[88] a) R. Dronskowski, K. Korczak, H. Lueken, W. Jung, *Angew. Chem. Int. Ed.* **2002**, *41*, 2528; b) B. P. T. Fokwa, H. Lueken, R. Dronskowski, *Chem. Eur. J.* **2007**, *13*, 6040; c) J. Brgoch, C. Goerens, B. P. T. Fokwa, G. J. Miller, *J. Am. Chem. Soc.* **2011**, *133*, 6832; d) Indeed, a systematic *in silico* scan of magnetic contrast in transition-metal doped PCMs has been reported: J. M. Skelton, S. R. Elliott, *J. Phys.: Condens. Matter* **2013**, *25*, 205801.
[89] V. L. Deringer, M. Lumeij, R. P. Stoffel, R. Dronskowski, *Chem. Mater.* **2013**, *25*, 2220.
[90] a) M. C. Payne, M. P. Teter, D. C. Allan, T. A. Arlas, J. D. Joannopoulos, *Rev. Mod. Phys.* **1992**, *64*, 1045; b) P. E. Blöchl, *Phys. Rev. B* **1994**, *50*, 17953; c) G. Kresse, D. Joubert, *Phys. Rev. B* **1999**, *59*, 1758.
[91] a) D. Sánchez-Portal, E. Artacho, J. M. Soler, *Solid State Commun.* **1995**, *95*, 685; b) M. D. Segall, R. Shah, C. J. Pickard, M. C. Payne, *Phys. Rev. B* **1996**, *54*, 16317; c) V. L. Deringer, A. L. Tchougréeff, R. Dronskowski, *J. Phys. Chem. A* **2011**, *115*, 5461; d) B. D. Dunnington, J. R. Schmidt, *J. Chem. Theory Comput.* **2012**, *8*, 1902; e) T. R. Galeev, B. D. Dunnington, J. R. Schmidt, A. I. Boldyrev, *Phys. Chem. Chem. Phys.* **2013**, *15*, 5022.
[92] S. Maintz, V. L. Deringer, A. L. Tchougréeff, R. Dronskowski, *J. Comput. Chem.* **2013**, *34*, 2557.
[93] V. L. Deringer, R. Dronskowski, *Chem. Sci.* **2014**, *5*, 894.
[94] J. R. Errington, P. G. Debenedetti, *Nature* **2001**, *409*, 318.
[95] a) D. Ielmini, A. L. Lacaita, D. Mantegazza, *IEEE Trans. Electron Devices* **2007**, *54*, 308; b) P. Fantini, S. Brazzelli, E. Cazzini, A. Mani, *Appl. Phys. Lett.* **2012**, *100*, 013505; c) D. Krebs, R. M. Schmidt, J. Klomfaß, J. Luckas, G. Bruns, C. Schlockermann,

M. Salinga, R. Carius, M. Wuttig, *J. Non-Cryst. Solids* **2012**, *358*, 2412.
[96] a) C. J. Glassbrenner, G. A. Slack, *Phys. Rev.* **1963**, *134*, A1058; b) H. J. Goldsmid, M. M. Kaila, G. L. Paul, *Phys. Status Solidi (a)* **1983**, *76*, K31.
[97] W. P. Risk, C. T. Rettner, S. Raoux, *Appl. Phys. Lett.* **2009**, *94*, 101906.
[98] K. S. Siegert, F. R. L. Lange, E. R. Sittner, H. Volker, C. Schlockermann, T. Siegrist, M. Wuttig, *Rep. Prog. Phys.* **2015**, *78*, 013001.
[99] S. Lee, K. Esfarjani, T. Luo, J. Zhou, Z. Tian, G. Chen, *Nat. Commun.* **2014**, *5*, 3525.
[100] a) J. M. Yáñez-Limón, J. González-Hernández, J. J. Alvarado-Gil, I. Delgadillo, H. Vargas, *Phys. Rev. B* **1995**, *52*, 16321; b) L. E. Shelimova, O. G. Karpinskii, P. P. Konstantinov, M. A. Kretova, E. S. Avilov, V. S. Zemskov, *Inorg. Mater.* **2001**, *37*, 342; c) B.-S. Lee, J. R. Abelson, S. G. Bishop, D.-H. Kang, B.-K. Cheong, K.-B. Kim, *J. Appl. Phys.* **2005**, *97*, 093509.
[101] A. H. Edwards, A. C. Pineda, P. A. Schultz, M. G. Martin, A. P. Thompson, H. P. Hjalmarson, C. J. Umrigar, *Phys. Rev. B* **2006**, *73*, 045210.
[102] S. Caravati, M. Bernasconi, T. D. Kuehne, M. Krack, M. Parrinello, *J. Phys.: Condens. Matter* **2009**, *21*, 499803.
[103] T. Siegrist, P. Jost, H. Volker, M. Woda, P. Merkelbach, C. Schlockermann, M. Wuttig, *Nat. Mater.* **2011**, *10*, 202.
[104] W. Zhang, A. Thiess, P. Zalden, R. Zeller, P. H. Dederichs, J. Y. Raty, M. Wuttig, S. Blügel, R. Mazzarello, *Nat. Mater.* **2012**, *11*, 952.
[105] P. Nukala, R. Agarwal, X. Qian, M. H. Jang, S. Dhara, K. Kumar, A. T. C. Johnson, J. Li, R. Agarwal, *Nano Lett.* **2014**, *14*, 2201.
[106] S.-W. Nam, H.-S. Chung, Y. C. Lo, L. Qi, J. Li, Y. Lu, A. T. C. Johnson, Y. Jung, P. Nukala, R. Agarwal, *Science* **2012**, *336*, 1561.
[107] a) D. Yu, J. Wu, Q. Gu, H. Park, *J. Am. Chem. Soc.* **2006**, *128*, 8148; b) S. Meister, H. Peng, K. McIlwrath, K. Jarausch, X. F. Zhang, Y. Cui, *Nano Lett.* **2006**, *6*, 1514; c) H.-S. Chung, Y. Jung, S. C. Kim, D. H. Kim, K. H. Oh, R. Agarwal, *Nano Lett.* **2009**, *9*, 2395; d) Y. Jung, S.-H. Lee, D.-K. Ko, R. Agarwal, *J. Am. Chem. Soc.* **2006**, *128*, 14026.
[108] a) M.-K. Lee, T. G. Kim, B.-K. Ju, Y.-M. Sung, *Cryst. Growth Des.* **2009**, *9*, 938; b) M. R. Buck, I. T. Sines, R. E. Schaak, *Chem. Mater.* **2010**, *22*, 3236; c) M. J. Polking, H. Zheng, R. Ramesh, A. P. Alivisatos, *J. Am. Chem. Soc.* **2011**, *133*, 2044; d) I. U. Arachchige, R. Soriano, C. D. Malliakas, S. A. Ivanov, M. G. Kanatzidis, *Adv. Funct. Mater.* **2011**, *21*, 2737.
[109] R. Hoffmann, *Angew. Chem. Int. Ed.* **2013**, *52*, 93.
[110] M. A. Caldwell, R. G. D. Jeyasingh, H.-S. P. Wong, D. J. Milliron, *Nanoscale* **2012**, *4*, 4382.
[111] T. C. Chong, L. P. Shi, R. Zhao, P. K. Tan, J. M. Li, H. K. Lee, X. S. Miao, A. Y. Du, C. H. Tung, *Appl. Phys. Lett.* **2006**, *88*, 122114.
[112] R. E. Simpson, P. Fons, A. V. Kolobov, T. Fukaya, M. Krbal, T. Yagi, J. Tominaga, *Nat. Nanotechnol.* **2011**, *6*, 501.
[113] H. Yang, C. T. Chong, R. Zhao, H. K. Lee, J. Li, K. G. Lim, L. Shi, *Appl. Phys. Lett.* **2009**, *94*, 203110.
[114] A. V. Kolobov, D. J. Kim, A. Giussani, P. Fons, J. Tominaga, R. Calarco, A. Gruverman, *APL Mater.* **2014**, *2*, 066101.
[115] G. S. Pawley, W. Cochran, R. A. Cowley, G. Dolling, *Phys. Rev. Lett.* **1966**, *17*, 753.
[116] D. J. Gravesteijn, H. M. van Tongeren, M. Sens, T. Bertens, C. J. van der Poel, *Appl. Opt.* **1987**, *26*, 4772.
[117] S. Raoux, A. K. König, H.-Y. Cheng, D. Garbin, R. W. Cheek, J. L. Jordan-Sweet, M. Wuttig, *Phys. Status Solidi (b)* **2012**, *249*, 1999.
[118] T. G. Edwards, I. Hung, Z. Gan, B. Kalkan, S. Raoux, S. Sen, *J. Appl. Phys.* **2013**, *114*, 233512.
[119] a) J. Kalikka, J. Akola, R. O. Jones, *J. Phys.: Condens. Matter* **2013**, *25*, 115801; b) J. A. Dixon, S. R. Elliott, *Appl. Phys. Lett.* **2014**, *104*, 141905.
[120] K. Deneke, A. Rabenau, *Z. Anorg. Allg. Chem.* **1964**, *333*, 201.
[121] Y. Maeda, H. Andoh, I. Ikuta, H. Minemura, *J. Appl. Phys.* **1988**, *64*, 1715.
[122] T. Schröder, T. Rosenthal, S. Grott, C. Stiewe, J. de Boor, O. Oeckler, *Z. Anorg. Allg. Chem.* **2013**, *639*, 2536.
[123] Y. I. Kim, E. T. Kim, J. Y. Lee, Y. T. Kim, *Appl. Phys. Lett.* **2011**, *98*, 091915.
[124] H. J. Shin, Y.-S. Kang, A. Benayad, K.-H. Kim, Y. M. Lee, M.-C. Jung, T.-Y. Lee, D.-S. Suh, K. H. P. Kim, C. Kim, Y. Khang, *Appl. Phys. Lett.* **2008**, *93*, 021905.
[125] a) J. C. Phillips, J. A. van Vechten, *Phys. Rev. Lett.* **1969**, *22*, 705; b) J. St. John, A. N. Bloch, *Phys. Rev. Lett.* **1974**, *33*, 1095; c) A. Zunger, *Phys. Rev. Lett.* **1980**, *44*, 582; d) P. B. Littlewood, *J. Phys. C: Solid State Phys.* **1980**, *13*, 4855.
[126] M. Wuttig, S. Raoux, *Z. Anorg. Allg. Chem.* **2012**, *638*, 2455.
[127] M. Luo, M. Wuttig, *Adv. Mater.* **2004**, *16*, 439.
[128] P. Hosseini, C. D. Wright, H. Bhaskaran, *Nature* **2014**, *511*, 206.
[129] a) A.-K. U. Michel, D. N. Chigrin, T. W. W. Maß, K. Schönauer, M. Salinga, M. Wuttig, T. Taubner, *Nano Lett.* **2013**, *13*, 3470; b) B. Gholipour, J. Zhang, K. F. MacDonald, D. W. Hewak, N. I. Zheludev, *Adv. Mater.* **2013**, *25*, 3050; c) L. Zou, M. Cryan, M. Klemm, *Opt. Express* **2014**, *22*, 24142.
[130] H. Zhang, C.-X. Liu, X.-L. Qi, X. Dai, Z. Fang, S.-C. Zhang, *Nat. Phys.* **2009**, *5*, 438.
[131] M. Z. Hasan, C. L. Kane, *Rev. Mod. Phys.* **2010**, *82*, 3045.
[132] J. Kim, J. Kim, S.-H. Jhi, *Phys. Rev. B* **2010**, *82*, 201312(R).
[133] B. Sa, J. Zhou, Z. Sun, R. Ahuja, *Europhys. Lett.* **2012**, *97*, 27003.
[134] a) F. Yan, T. J. Zhu, X. B. Zhao, S. R. Dong, *Appl. Phys. A* **2007**, *88*, 425; b) M. N. Schneider, T. Rosenthal, C. Stiewe, O. Oeckler, *Z. Kristallogr.* **2010**, *225*, 463; c) E.-R. Sittner, K. S. Siegert, P. Jost, C. Schlockermann, F. R. L. Lange, M. Wuttig, *Phys. Status Solidi (a)* **2013**, *210*, 147.
[135] G. J. Snyder, E. S. Toberer, *Nat. Mater.* **2008**, *7*, 105.
[136] S. R. Ovshinsky, *Jpn. J. Appl. Phys.* **2004**, *43*, 4695.
[137] a) C. D. Wright, Y. Liu, K. I. Kohary, M. M. Aziz, R. J. Hicken, *Adv. Mater.* **2011**, *23*, 3408; b) D. Kuzum, R. G. D. Jeyasingh, B. Lee, H.-S. P. Wong, *Nano Lett.* **2012**, *12*, 2179.